PRIN NAT-NET Virtual Meeting
6th July 2021

WP3
SOURCES AND FLUXES OF NEUTRINOS AND OTHER MESSENGERS

- Relic neutrino detection
- Axions and ALP in astrophysical context
- Issues in BBN neutrinos
- HE neutrinos and MM approach
- Solar neutrino models and low-energy flux detection
- Reference geo-neutrino models
- Core-collapse SN physics

Conveners
Alessandro MIRIZZI
Giulia PAGLIAROLI

The Role of Unresolved PWNe to the Gamma-ray Diffuse Emission at GeV

Vittoria Vecchiotti

Gran Sasso Science Institute, Italy

In collaboration with: M. Cataldo, G. Pagliaroli and F. L. Villante

Based on: **Cataldo et al. *Astrophys.J.* 904 (2020)** , https://doi.org/10.21203/rs.3.rs-539249/v1

Outline:

- Pulsar Wind Nebulae (1-100 TeV)
- The contribution of PWNe (1-100 GeV)
- The Fermi Unresolved PWNe
- Ring analysis of the diffuse gamma emission

Prediction on the Pulsar wind nebulae population in the TeV range:

Cataldo et al. ***Astrophys.J.*** **904 (2020)**

- The HGPS catalogue ($\phi > 0.1\phi_{Crab}$);
- Model for TeV source population based on the assumption of the spatial distribution and the luminosity distribution of the sources;

$$\frac{dN}{d^3r\,dL} = \rho(r)Y(L)$$

Lorimer et al. 2006

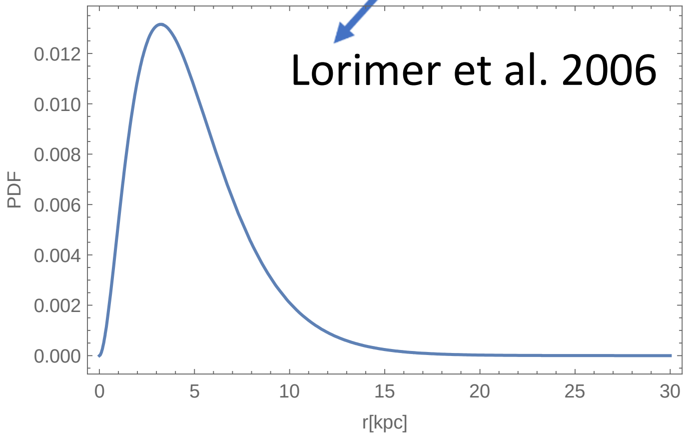

$$\boxed{Y(L) = \frac{R\,\tau\,(\alpha-1)}{L_{\max}}\left(\frac{L}{L_{\max}}\right)^{-\alpha}}$$

$$\alpha = 1/\gamma + 1$$

$$R = 0.019\,\mathrm{yr}^{-1}$$

For pulsar-powered sources:

$$L(t) = L_{\max}\left(1+\frac{t}{\tau}\right)^{-\gamma}$$

Abdalla et al, *A&A*, 612, A1 (2018)

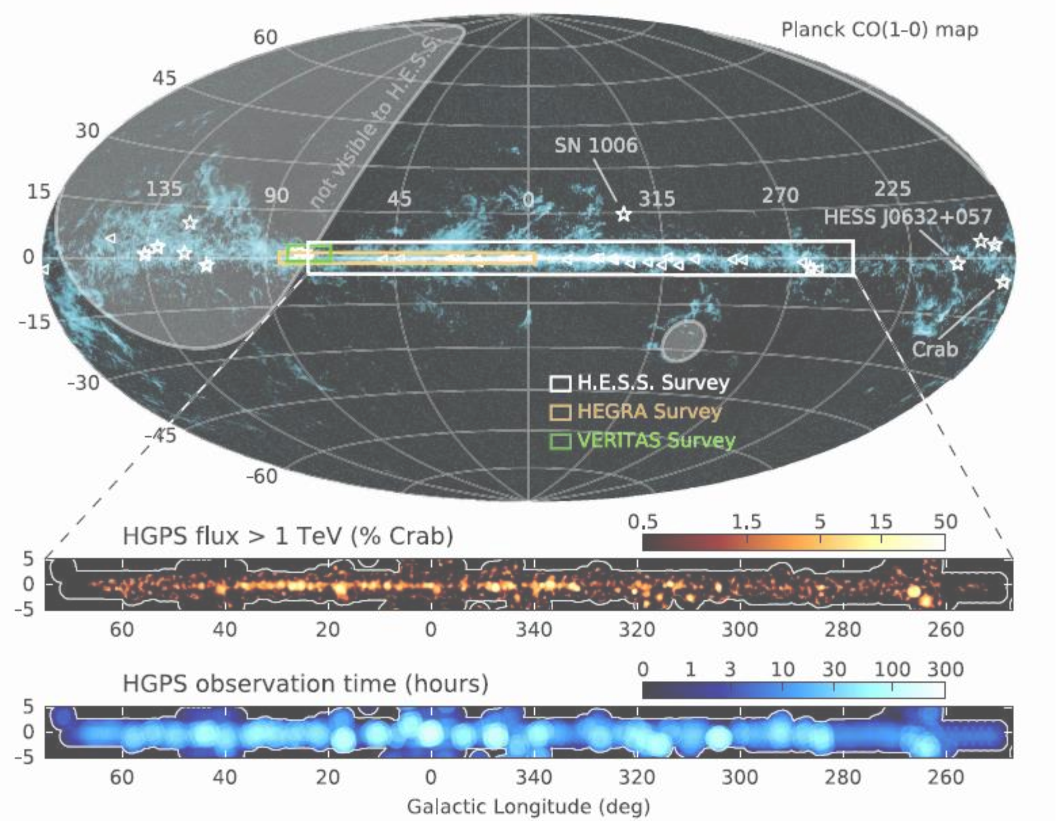

Prediction on the Pulsar wind nebulae population in the TeV range:

We assumed a **power-law** energy spectrum with index $\boldsymbol{\beta_{TeV} = 2.3}$ that is the average index of the catalogue for all the sources.

Cataldo et al. *Astrophys.J.* 904 (2020)

$\alpha = 1.8$

$$\boxed{\begin{aligned} L_{max} &= 6.8 \times 10^{35}\ erg\ s^{-1} \\ \tau &= 0.5\ kyr \end{aligned}}$$

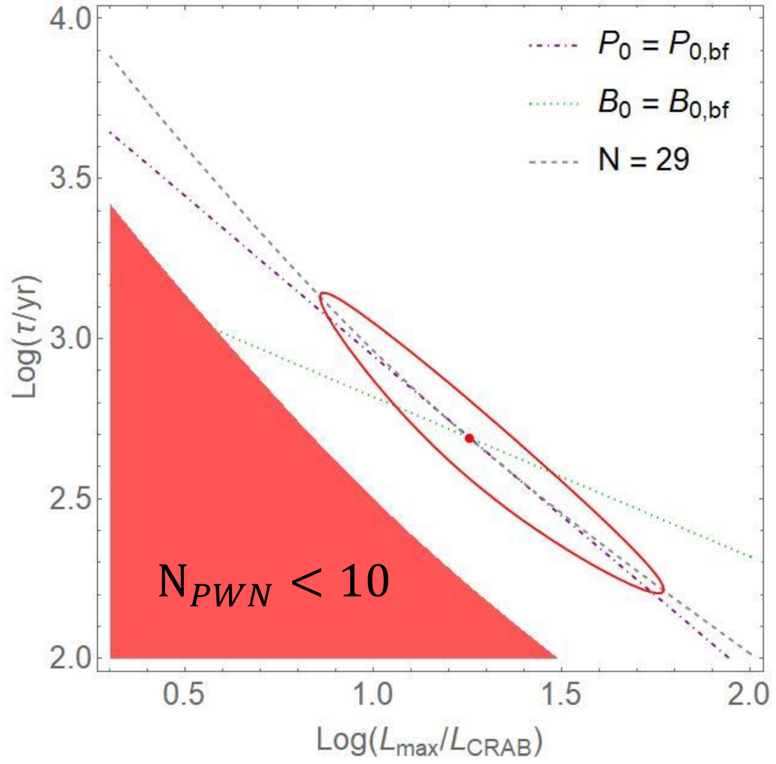

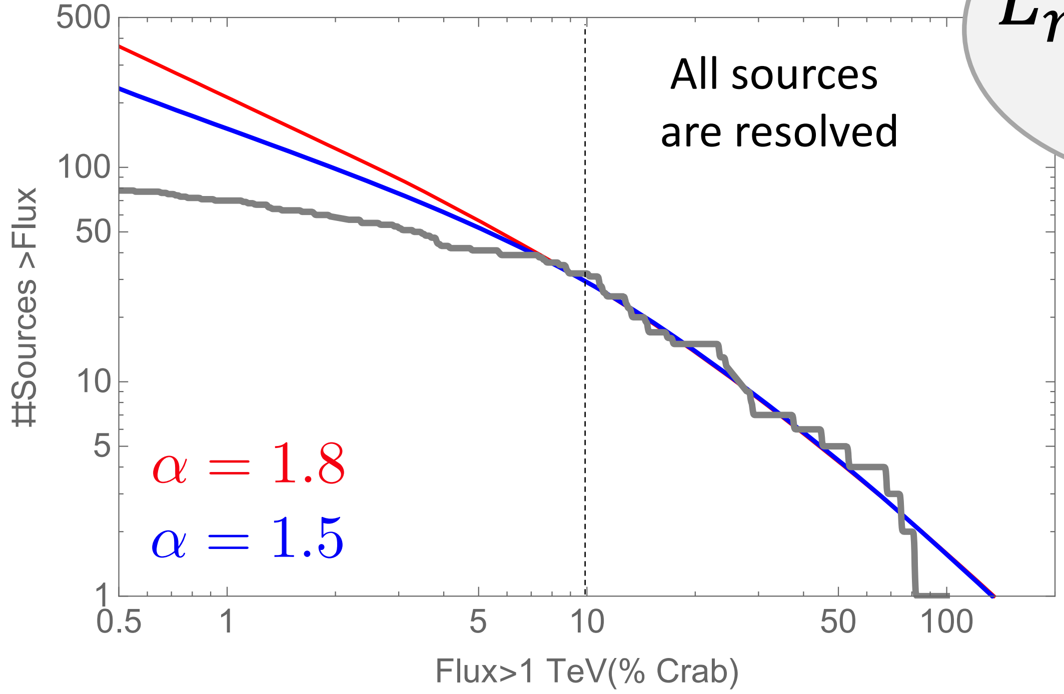

$$L_{max} = L^{BF}$$
$$\tau = \tau^{BF}$$

$$\boxed{\Phi_{\mathrm{PWN}}}$$

Total flux due to PWNe in the FERMI energy range (1-100 GeV)?

Extrapolate to GeV range:

- Spectral assumption: broken power-law:

$$\varphi_{\rm PWN}(E) = \varphi_0 \left\{ \begin{array}{ll} \left(\frac{E}{E_b}\right)^{-\beta_{GeV}} & E \leq E_b \\ \left(\frac{E}{E_b}\right)^{-\beta_{TeV}} & E > E_b \end{array} \right.$$

$E_b = 300\ GeV \qquad \beta_{GeV} < 2. \qquad \beta_{TeV} = 2.3$

PWNe Unresolved contribution (1-100 GeV):

$$\frac{\phi_{NR}}{\phi_{PWN}} = (46\% - 40\%)$$

$\alpha = 1.8$

A relevant fraction of the TeV PWNe population cannot be resolved by Fermi-LAT

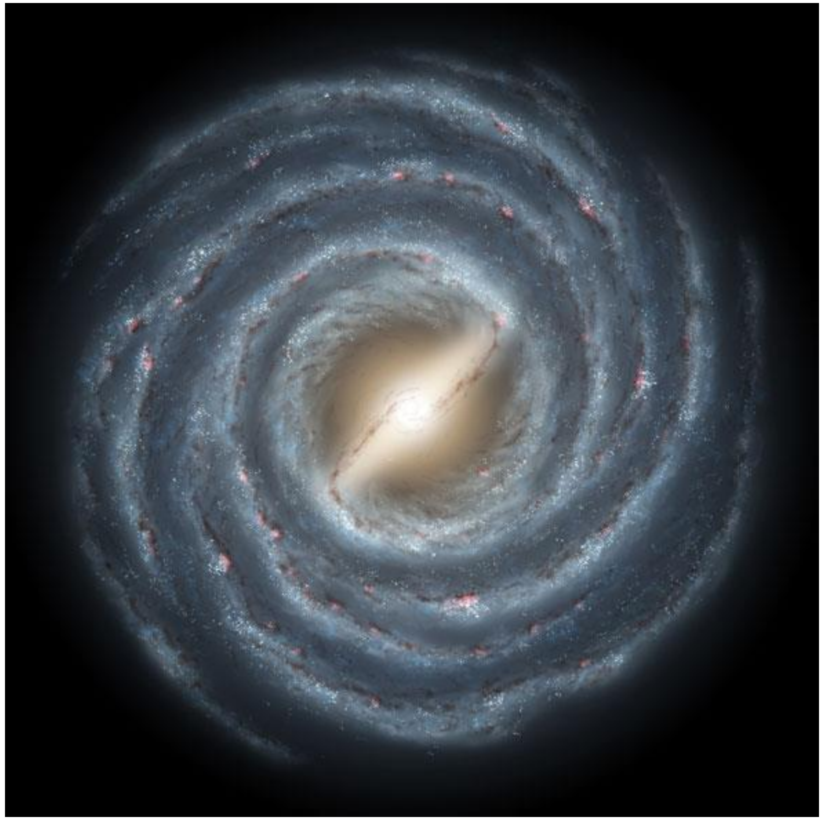

PWNe contribution in galactocentric rings

Table 1. *The cumulative flux of resolved (Φ^{R}_{GeV}) and unresolved (Φ^{NR}_{GeV}) TeV PWNe in the GeV domain for $\alpha = 1.8$ and for the two different values of R_Φ considered in our analysis. The Fermi-LAT diffuse emission Φ^{diff}_{GeV} is shown in the first column (Pothast et al. 2018). The numbers in brackets give the ratios $\Phi^{NR}_{GeV}/\Phi^{diff}_{GeV}$ in different galactocentric rings.*

	Φ^{diff}_{GeV} $(cm^{-2}\ s^{-1})$	Φ^{NR}_{GeV} $(cm^{-2}\ s^{-1})$		Φ^{R}_{GeV} $(cm^{-2}\ s^{-1})$	
		$R_\Phi = 500$	$R_\Phi = 1000$	$R_\Phi = 500$	$R_\Phi = 1000$
1.7 – 4.5 kpc	3.86×10^{-7}	6.63×10^{-8} (17%)	1.15×10^{-7} (29.9%)	2.78×10^{-8}	7.29×10^{-8}
4.5 – 5.5 kpc	3.11×10^{-7}	3.8×10^{-8} (12.2%)	6.62×10^{-8} (21.2%)	2.1×10^{-8}	5.2×10^{-8}
5.5 – 6.5 kpc	5.09×10^{-7}	4.24×10^{-8} (8.3%)	7.37×10^{-8} (14.4%)	3.0×10^{-8}	7.14×10^{-8}
6.5 – 7.0 kpc	2.57×10^{-7}	2.28×10^{-8} (8.8%)	3.96×10^{-8} (15.3%)	2.08×10^{-8}	4.77×10^{-8}
7.0 – 8.0 kpc	7.7×10^{-7}	5.29×10^{-8} (6.8%)	9.21×10^{-8} (11.9%)	7.03×10^{-8}	1.54×10^{-7}
8.0 – 10.0 kpc	3.84×10^{-6}	9.69×10^{-8} (2.5%)	1.68×10^{-7} (4.3%)	2.24×10^{-7}	4.74×10^{-7}
10.0 – 16.5 kpc	7.68×10^{-7}	3.0×10^{-8} (3.9%)	5.24×10^{-8} (6.8%)	1.9×10^{-8}	4.56×10^{-8}
16.5 – 50.0 kpc	4.44×10^{-8}	7.73×10^{-10} (1.7%)	1.38×10^{-9} (3.1%)	9.23×10^{-11}	3.44×10^{-10}
0.0 – 50.0 kpc	6.89×10^{-6}	3.55×10^{-7}(5.1%)	6.18×10^{-7} (8.9%)	4.15×10^{-7}	9.23×10^{-7}

9 Galactocentric rings

Total diffuse emission: 9.3 years of Fermi-LAT Pass 8 data (0.34−228.65) GeV and (|l|<180∘) and |b|<20.25∘

Diffuse emission due to unresolved PWNe (1-100) GeV

Resolved flux due to PWNe

Reinterpreting the diffuse emission observed by Fermi:

Truly diffuse (Power-Law):

$$\Gamma_1 = 2.56$$

Truly diffuse (Power-Law)
+ Uresolved PWNe

$$\Gamma_{BF} = 2.72$$

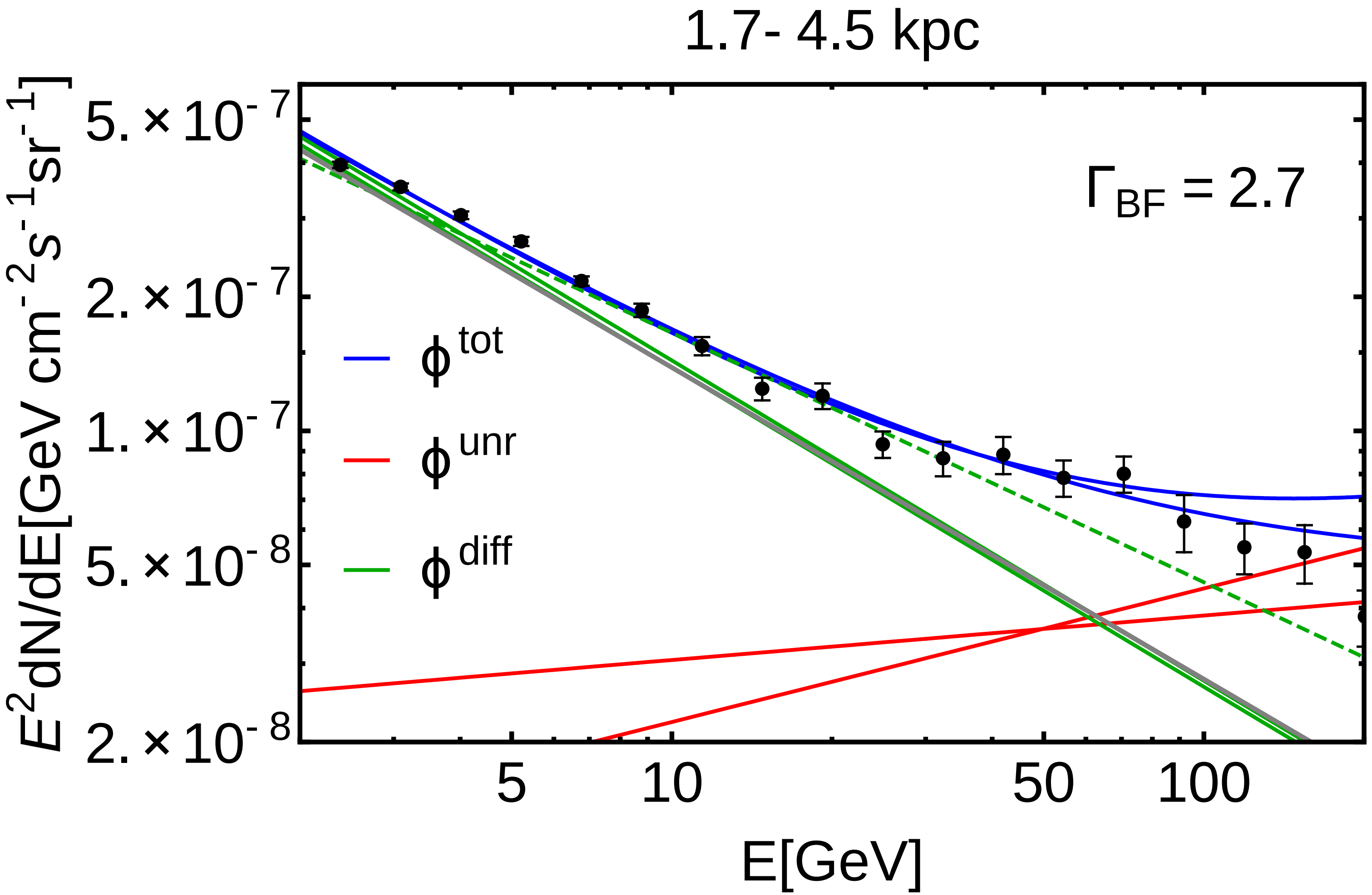

Spectral index of the truly diffuse emission::

Ring	Γ_1	Γ_{BF} $R_\Phi = 500$	$\alpha = 1.8$ $R_\Phi = 1000$
1.7 – 4.5 kpc	2.56 ± 0.02	2.72 ± 0.01	2.72 ± 0.01
4.5 – 5.5 kpc	2.48 ± 0.02	2.57 ± 0.01	2.56 ± 0.01
5.5 – 6.5 kpc	2.54 ± 0.04	2.63 ± 0.01	2.63 ± 0.01
6.5 – 7 kpc	2.54 ± 0.01	2.62 ± 0.01	2.61 ± 0.02
7 – 8 kpc	2.57 ± 0.01	2.625 ± 0.008	2.623 ± 0.008
8 – 10 kpc	2.642 ± 0.003	2.663 ± 0.003	2.662 ± 0.004
10 – 16.5 kpc	2.696 ± 0.008	2.743 ± 0.008	2.740 ± 0.009
16.5 – 50 kpc	2.72 ± 0.03	2.77 ± 0.04	2.76 ± 0.03

Truly diffuse (Power-Law)

Truly diffuse (Power-Law) + Uresolved PWNe

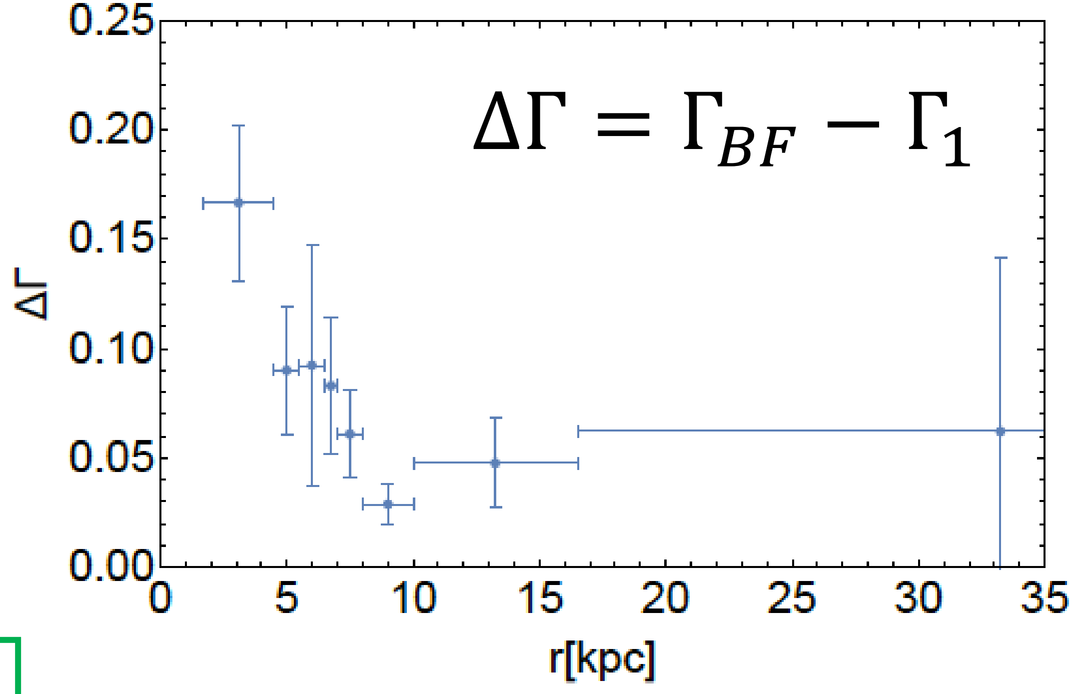

PWNe contribution accounts for a large part of the spectral index variation observed by Fermi-LAT, weakening the evidence of CR spectral hardening in the inner Galaxy

Summary:

- A relevant fraction of the TeV PWNe population cannot be resolved by Fermi-LAT
- The γ-ray flux due to unresolved TeV PWNe and the truly diffuse emission, due to CRs interactions with the interstellar gas, add up contributing to shape the radial and spectral behaviour of the total diffuse γ-ray emission observed by Fermi-LAT
- This additional component naturally accounts for a large part of the spectral index variation observed by Fermi-LAT, weakening the evidence of CR spectral hardening in the inner Galaxy

Joint Analysis Method on Gravitational Waves and Low-Energy Neutrinos to Detect Core-Collapse Supernovae

Odysse Halim[1,*], Claudio Casentini[2], Marco Drago[3,4], Viviana Fafone[5,6], Kate Scholberg[7], Carlo Vigorito[8,9], Giulia Pagliaroli[10,11]

1. INFN Trieste, Italy
2. INAF-IAPS, Rome, Italy
3. Univ of Rome "La Sapienza", Italy
4. INFN Rome, Italy
5. Univ. of Rome Tor Vergata, Italy
6. INFN Rome Tor Vergata, Italy
7. Trinity College of Arts & Sciences, Duke University, Durham, NC, USA
8. Univ. of Turin, Italy
9. INFN Torino, Italy
10. GSSI, L'Aquila, Italy
11. INFN LNGS, Assergi, Italy

* corresponding author

VIRGO

INFN TRIESTE

GOAL AND SCHEME

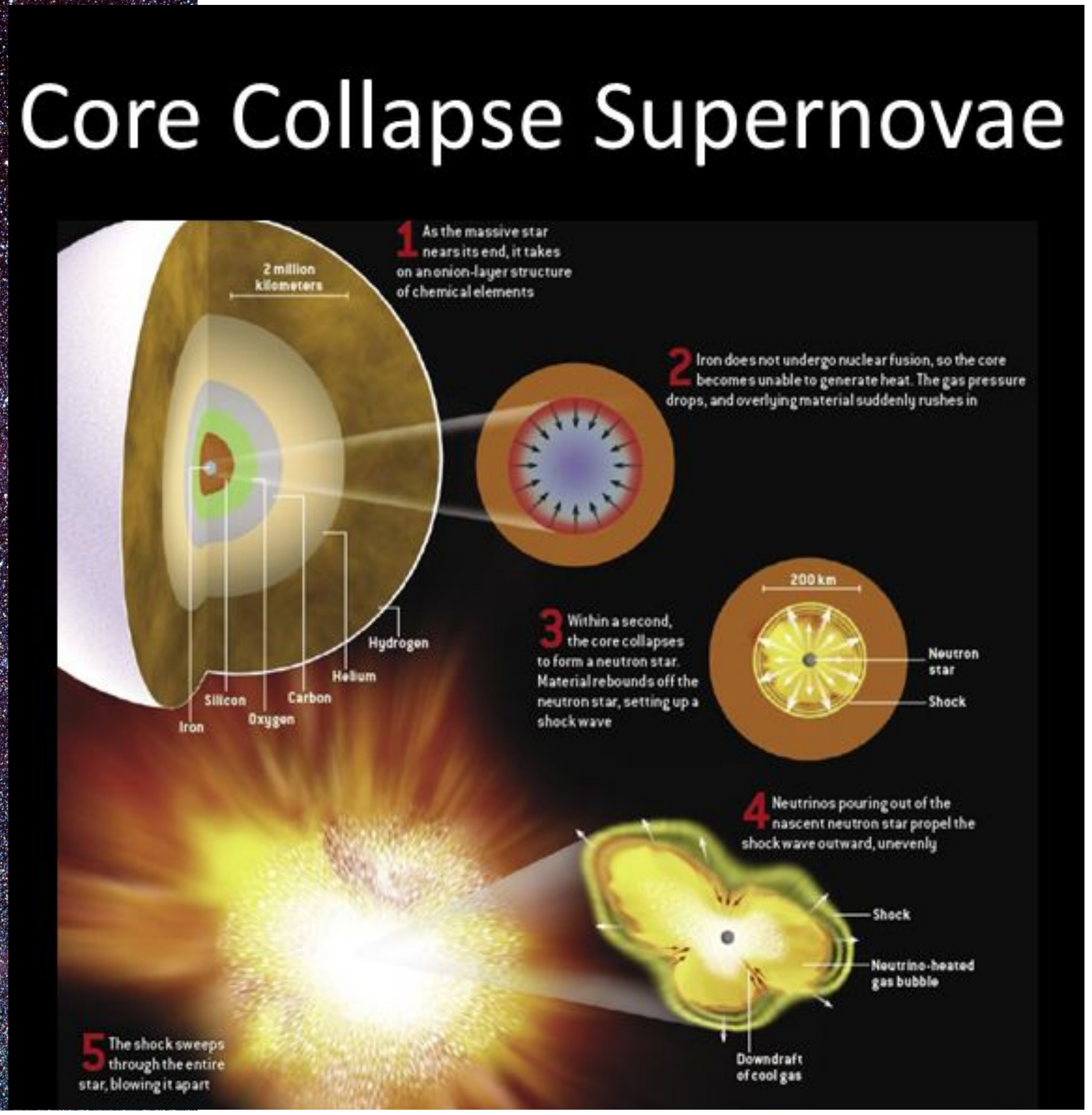

SN1987A. Credit: ESO

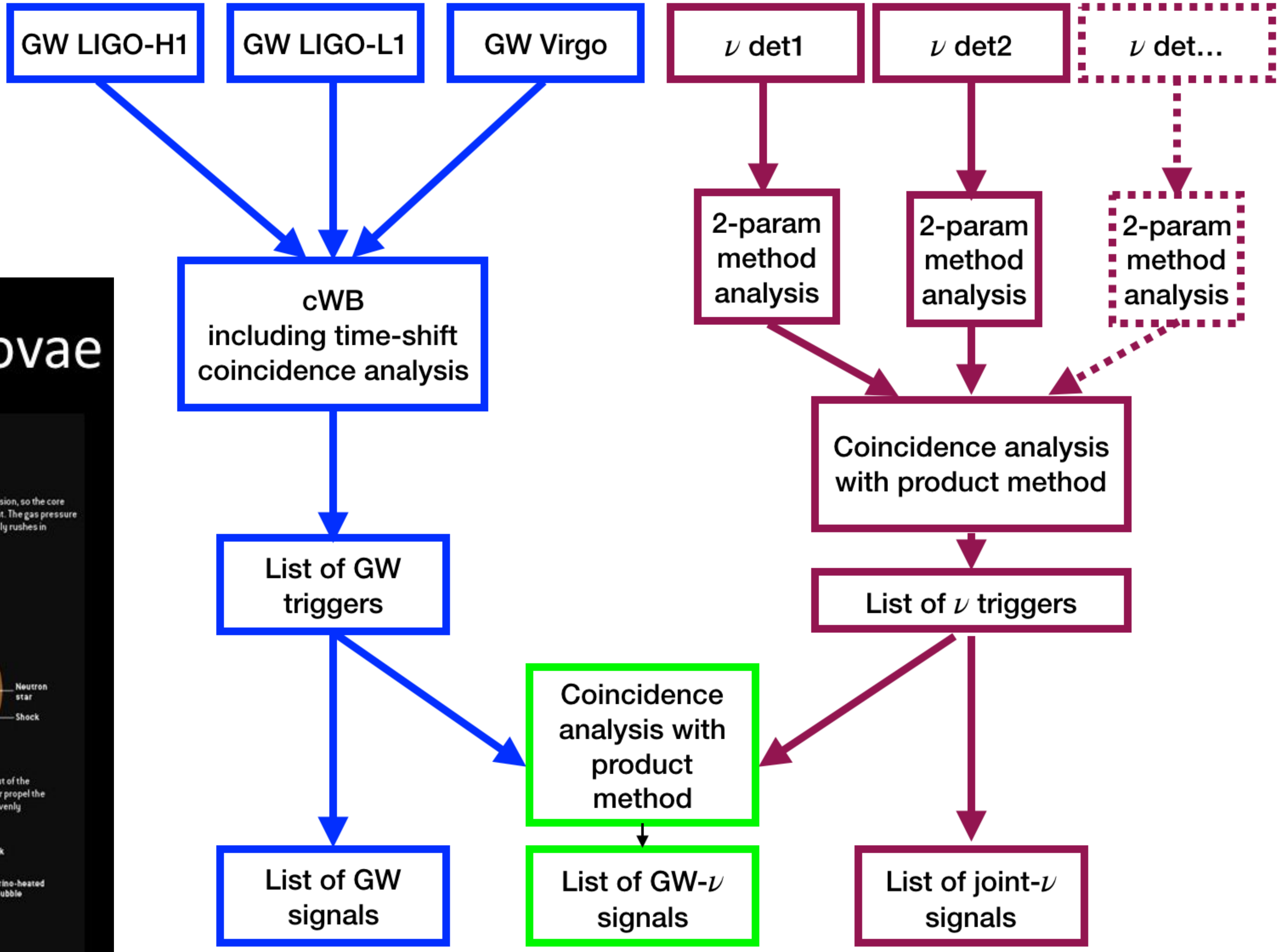

MESSENGERS AND WAVEFORM MODELS: GRAVITATIONAL WAVES

- Neutrino-radiation hydrodynamics (Rad) versus rapid rotation + magnetic field (Dim & Sch)

TABLE I: Waveforms from CCSN simulations used in this work. We report in the columns: emission type and reference, waveform identifier, waveform abbreviation in this manuscript, progenitor mass, angle-averaged root-sum-squared strain h_{rss}, frequency at which the GW energy spectrum peaks, and emitted GW energy.

Waveform Family	Waveform Identifier	Abbreviation	Mass $M_\odot$	h_{rss} @10 kpc $(10^{-22}\,1/\sqrt{\text{Hz}})$	f_{peak} [Hz]	E_{GW} $[10^{-9}\,M_\odot c^2]$
Radice [34] 3D simulation; h_+ and $h_\times$ (Rad)	s25	Rad25	25	0.141	1132	28
	s13	Rad13	13	0.061	1364	5.9
	s9	Rad9	9	0.031	460	0.16
Dimmelmeier [35] 2D simulation; h_+ only (Dim)	dim1-s15A2O05ls	Dim1	15	1.052	770	7.685
	dim2-s15A2O09ls	Dim2	15	1.803	754	27.880
	dim3-s15A3O15ls	Dim3	15	2.690	237	1.380
Scheidegger [36] 3D simulation; h_+ and $h_\times$ (Sch)	sch1-R1E1CA$_L$	Sch1	15	0.129	1155	0.1509
	sch2-R3E1AC$_L$	Sch2	15	5.144	466	0.02249
	sch3-R4E1FC$_L$	Sch3	15	5.796	698	0.04023

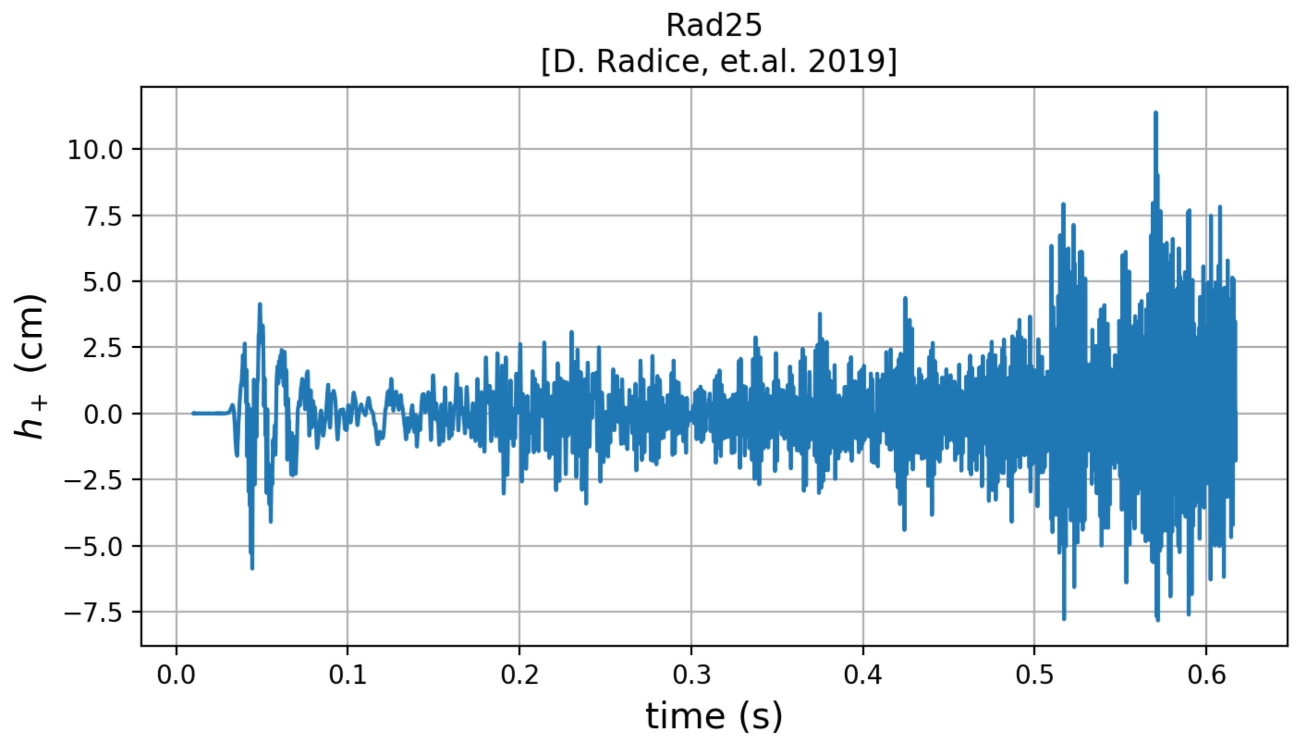

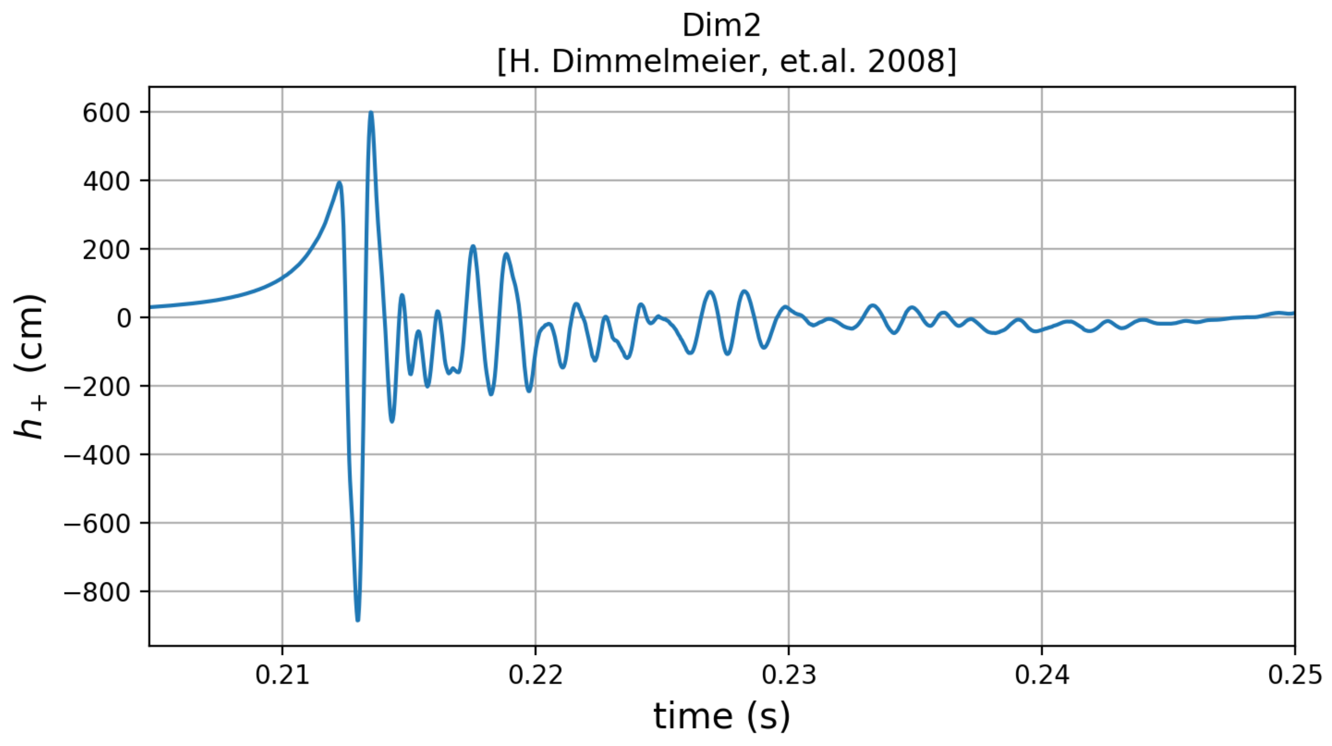

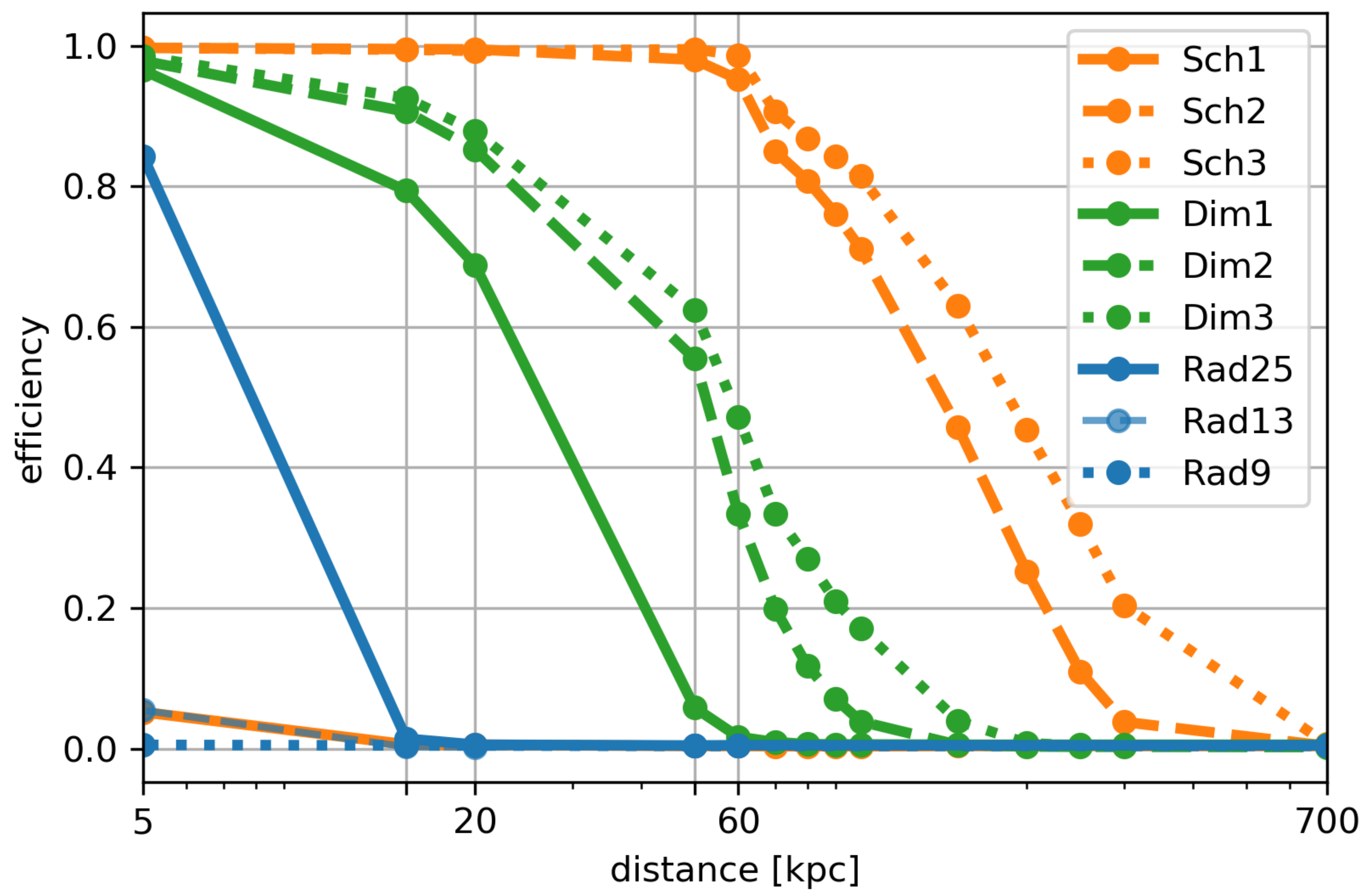

OH, et.al. 2021 *in preparation*

MESSENGERS AND WAVEFORM MODELS: LOW-ENERGY NEUTRINOS

TABLE II: Neutrino models and the expected number of events in the considered detectors (Super-K [4], LVD [5], and KamLAND [6]) with the assumed energy threshold ($E_{\rm thr}$).

Model (identifier)	Progenitor Mass	Super-K ($E_{\rm thr} = 6.5$ MeV)	LVD($E_{\rm thr} = 7$ MeV)	Kamland($E_{\rm thr} = 1$ MeV)
Pagliaroli [39] (SN1987A)	$25\,M_\odot$	4120	224	255
Hüdepohl [38] (Hud)	$11.2\,M_\odot$	2620	142	154

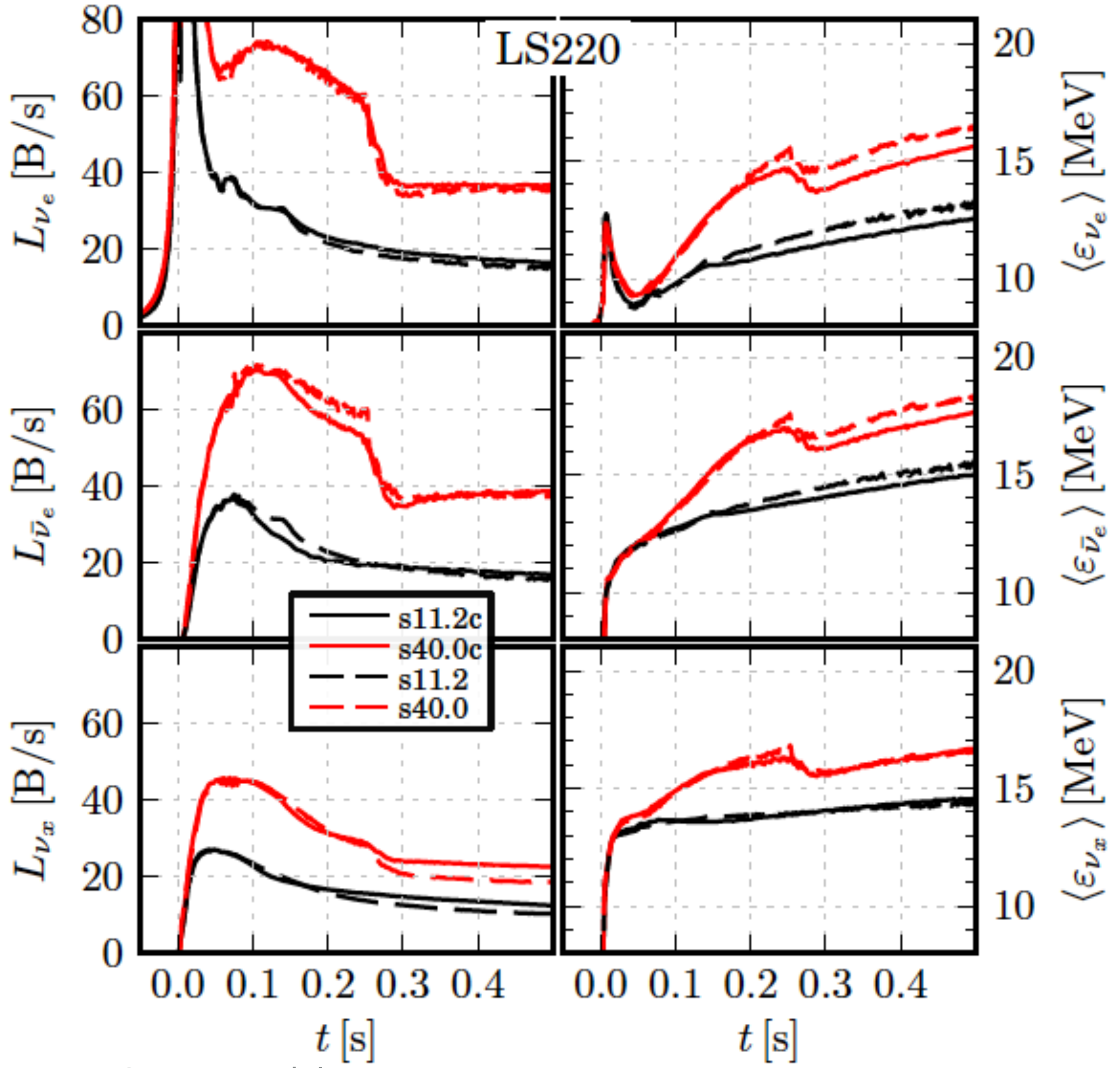

s11.2 is our model
L. Hudepohl, Ph.D. thesis, Technische Universitat Munchen (2014).

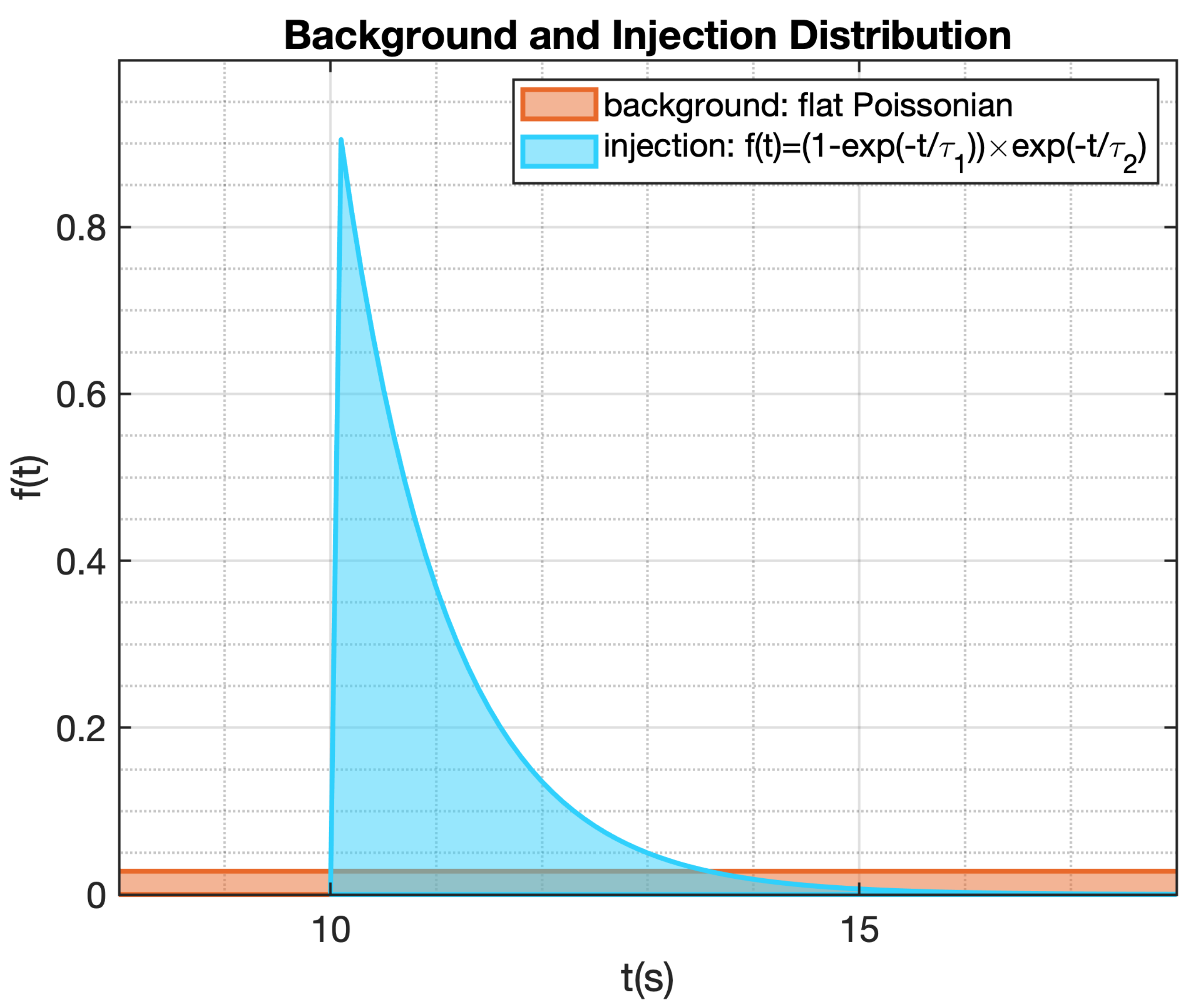

SN1987A model
OH, PhD thesis, Gran Sasso Science Institute (2020)

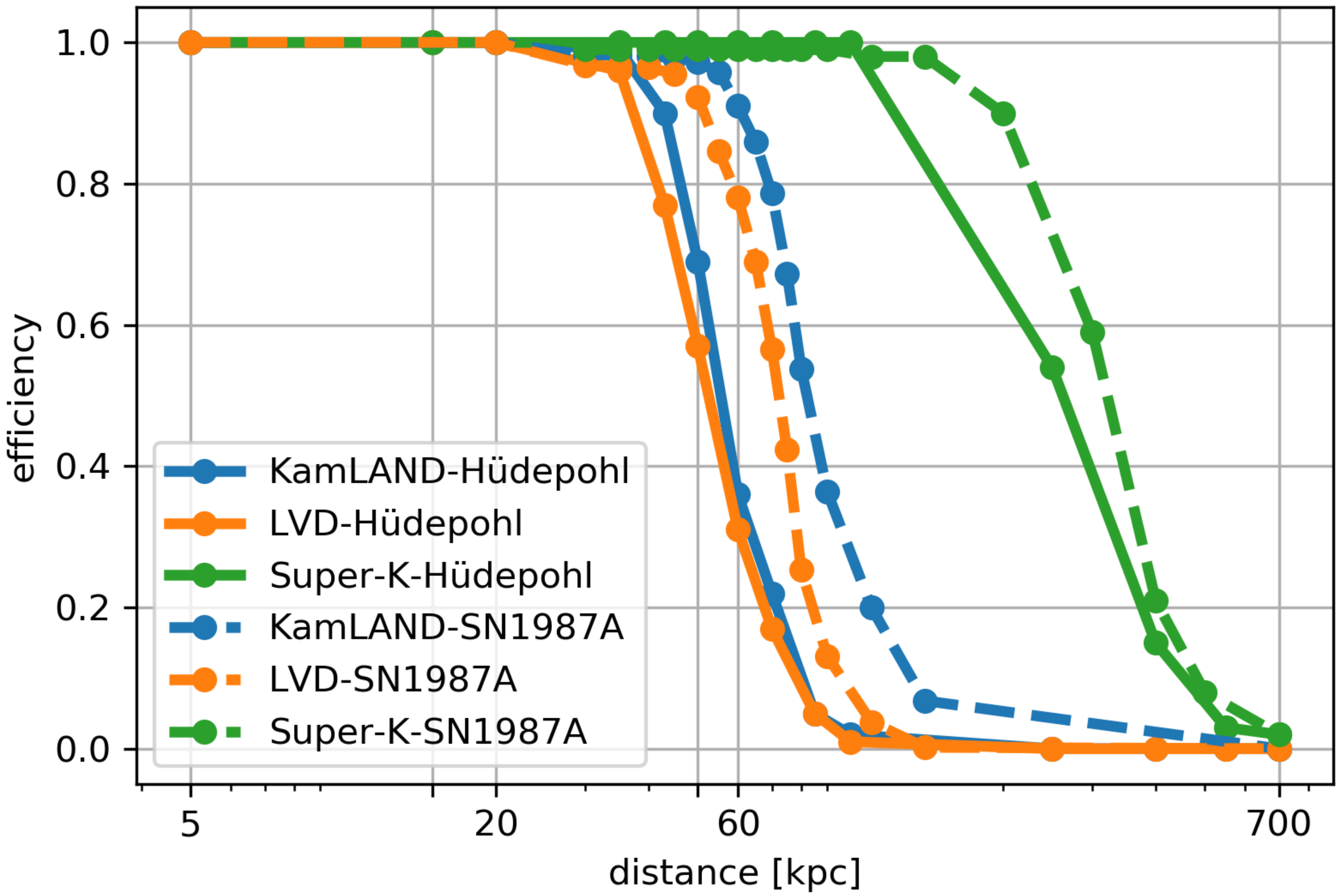

OH, et.al. 2021 *in preparation*

DATA AND ANALYSIS: LOW-ENERGY NEUTRINOS (OUR METHOD)

- Standard parameter: the **number** of events in a bin, ***multiplicity*** $\equiv m_i$
- A new parameter: behaviour of events (how close or well separated) in a bin, $\xi_i \equiv m_i/\Delta t_i$
    - Δt_i is the **duration**

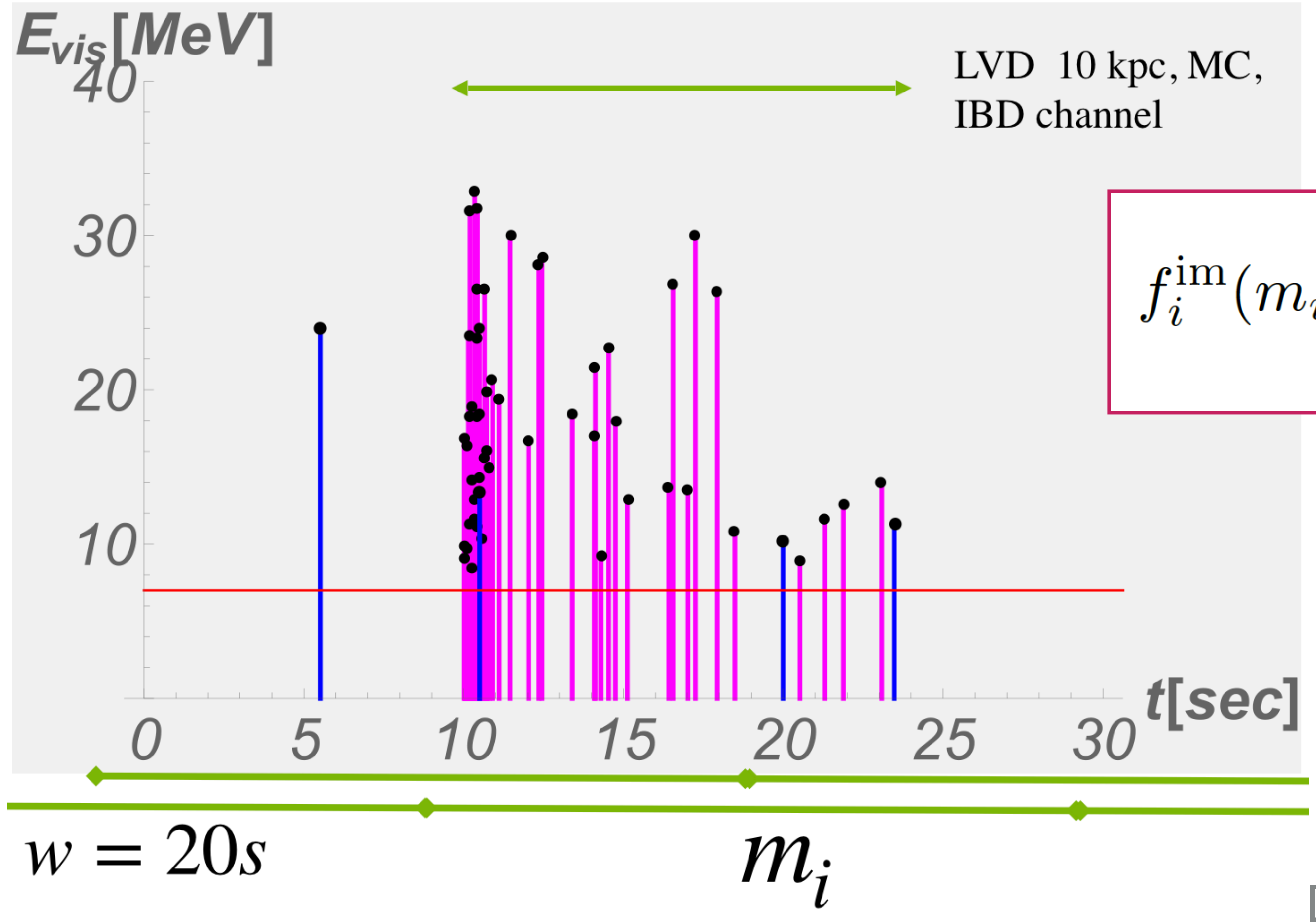

$$f_i^{\text{im}}(m_i) = N \times \sum_{k=m_i}^{\infty} P(k),$$

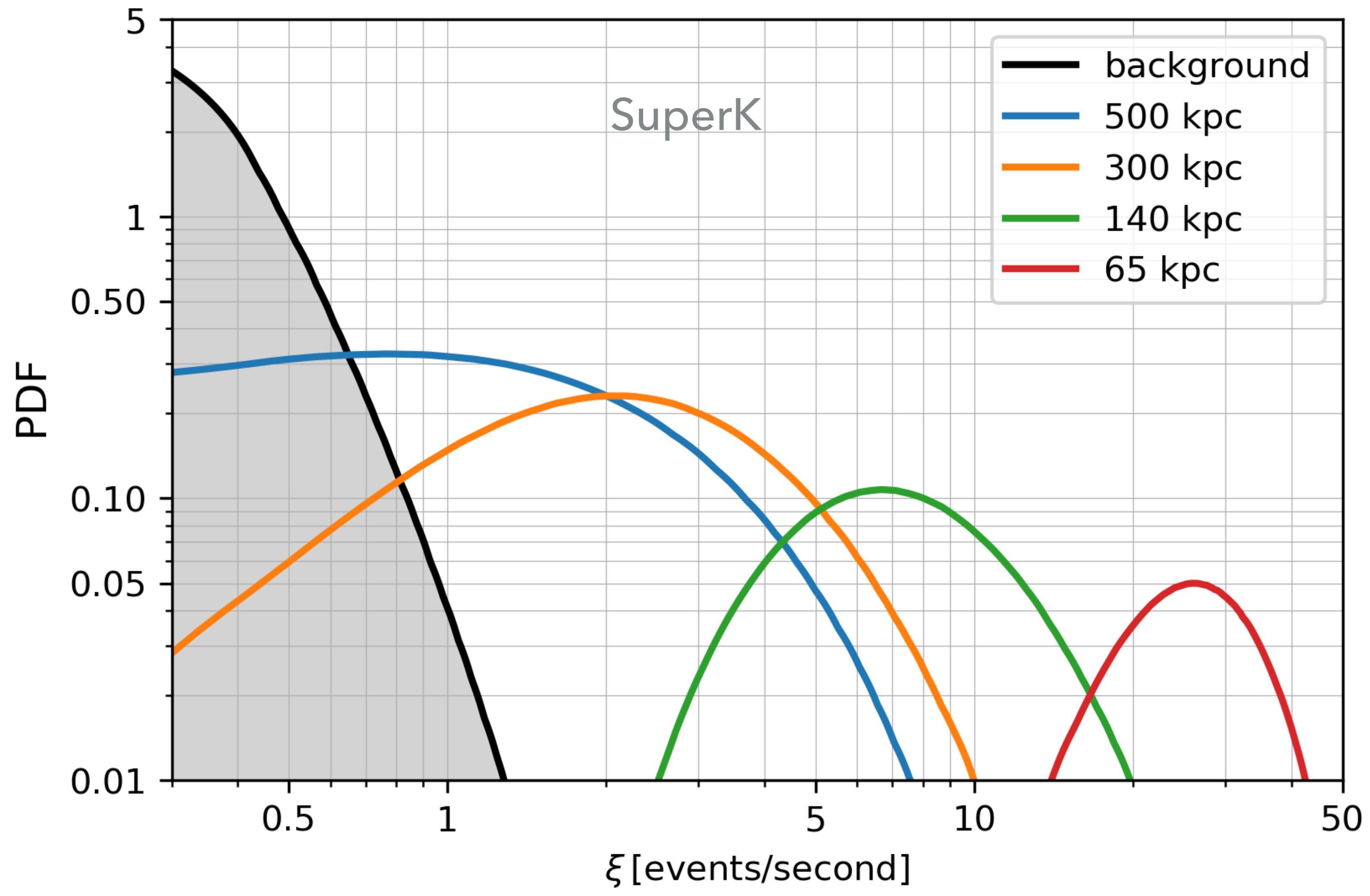

$$F_i^{\text{im}}(m_i, \xi_i) = N \times \sum_{k=m_i}^{\infty} P(k, \xi_i),$$

$$F_i^{\text{im}}(m_i, \xi_i) = N \times \sum_{k=m_i}^{\infty} P(k) \int_{\xi=\xi_i}^{\infty} \text{PDF}(\xi \geq \xi_i | k) d\xi.$$

Detailed formula: OH, PhD thesis, Gran Sasso Science Institute (2020)

DATA AND ANALYSIS: MULTIMESSENGER

- Single-detector neutrino threshold: 1/100 year in FAR
- Coincidence analysis threshold: 5σ (5.7×10^{-7}) in FAP

$$\mathrm{FAR}_\nu = \mathrm{Nd} \times w_\nu^{\mathrm{Nd}-1} \prod_{i=1}^{\mathrm{Nd}} F_i^{\mathrm{im}},$$

↓

$$\mathrm{FAR}_{\mathrm{glob}} = \mathrm{Net} \times w_c^{\mathrm{Net}-1} \prod_{X=1}^{\mathrm{Net}} \mathrm{FAR}_X,$$

↓

$$\mathrm{FAP} = 1 - e^{-\mathrm{FAR} \times \mathrm{livetime}},$$

RESULTS: 1-DETECTOR NEUTRINO

- SN1987A-signal model @60kpc injections, KamLAND detector model, 1/100yr FAR threshold

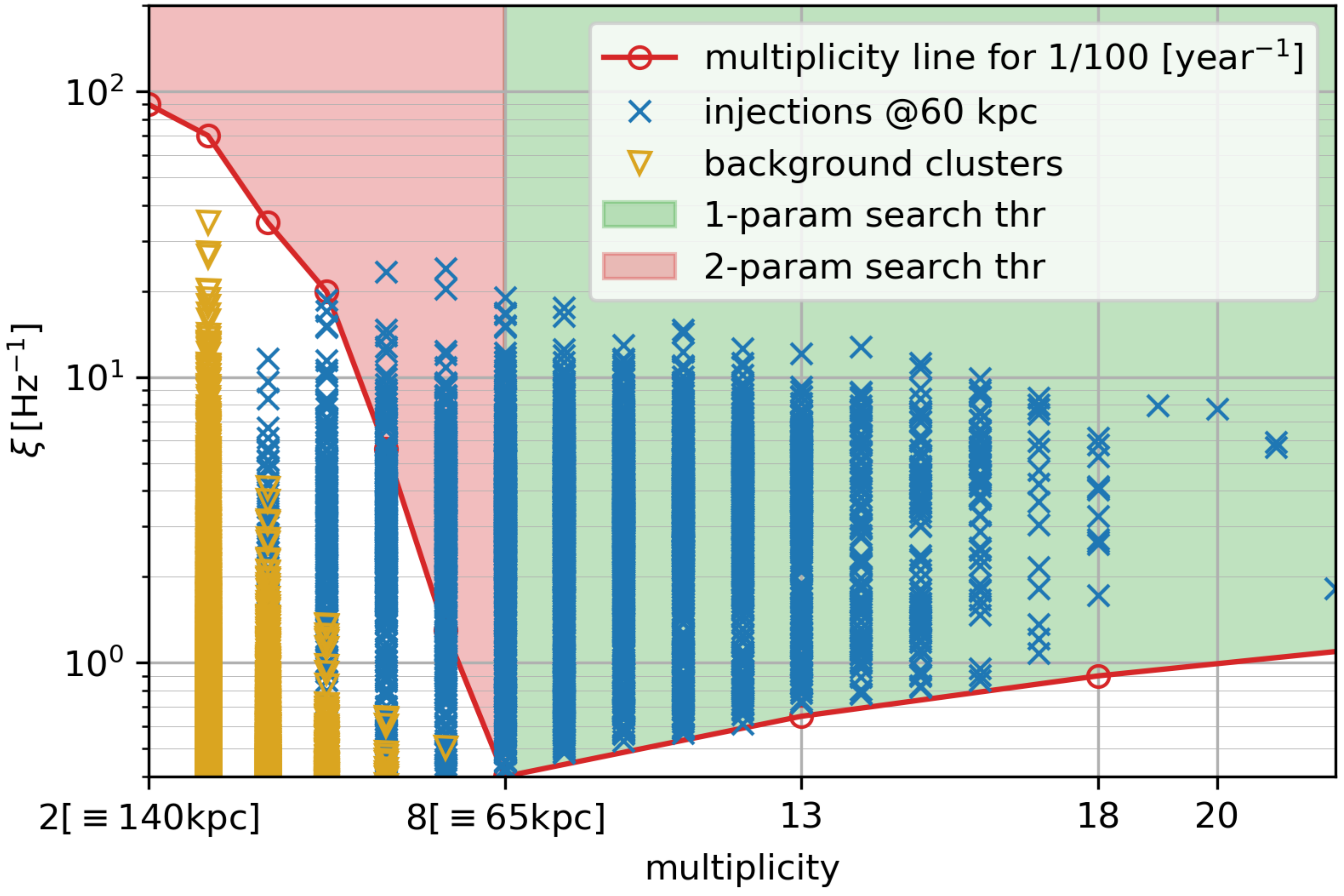

TABLE III: Efficiency (η) comparison between 1-parameter and 2-parameter method of single detector KamLAND 60-kpc for FAR$_\nu$ < 1/100 [year^{-1}] with SN1987A model.

Noise	Noise [< 1/100 yr]	η_{1param} [< 1/100 yr]	η_{2param} [< 1/100 yr]
75198	0/75198	2665/3654=**72.9%**	3026/3654=**82.8%**

OH, et.al. 2021 *in preparation*

RESULTS: SUB-NETWORK OF NEUTRINO DETECTORS

- Hüdepohl-signal model [5, 15, 20, 50, 60]-kpc injections, KamLAND+LVD detector model, 5σ-FAP threshold

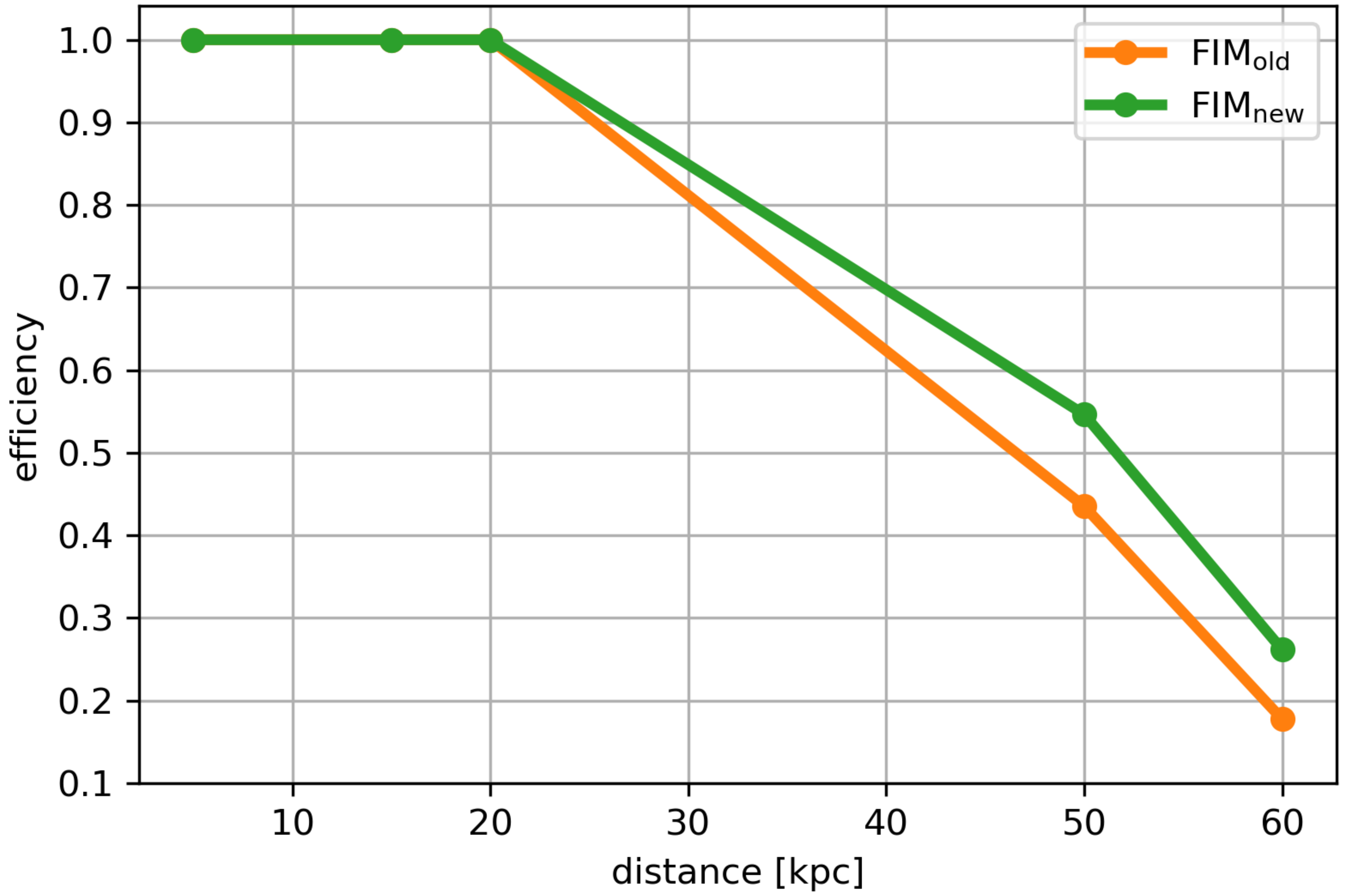

TABLE IV: Efficiency (η) comparison between 1-parameter and 2-parameter method for analysis of KamLAND-LVD with neutrino Hud model and for FAP$_\nu$ $> 5\sigma$.

Distance [kpc]	$\eta_{1\text{param}}$ [$> 5\sigma$]	$\eta_{2\text{param}}$ [$> 5\sigma$]
50	**47/108=43.5%**	**59/108=54.6%**
60	**19/107=17.8%**	**28/107=26.2%**

OH, et.al. 2021 *in preparation*

RESULTS: GLOBAL-NETWORK OF MULTIMESSENGERS

- SN1987A-signal model @60kpc injections, KamLAND and LVD detector model, 5σ-FAP threshold
- Dimmelmeier2-GW model @60kpc injections, [LIGO-H, LIGO-L, Virgo] detectors

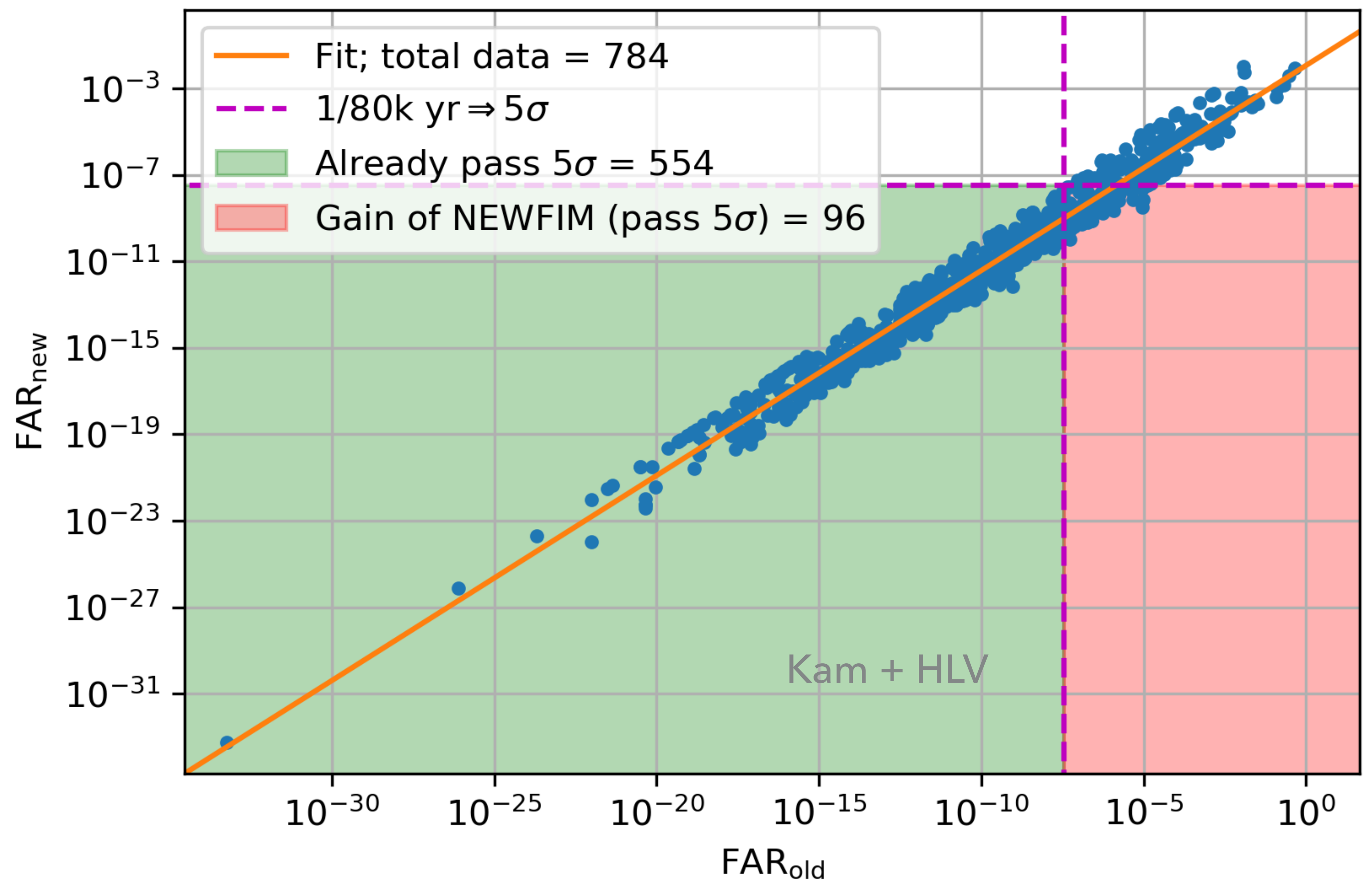

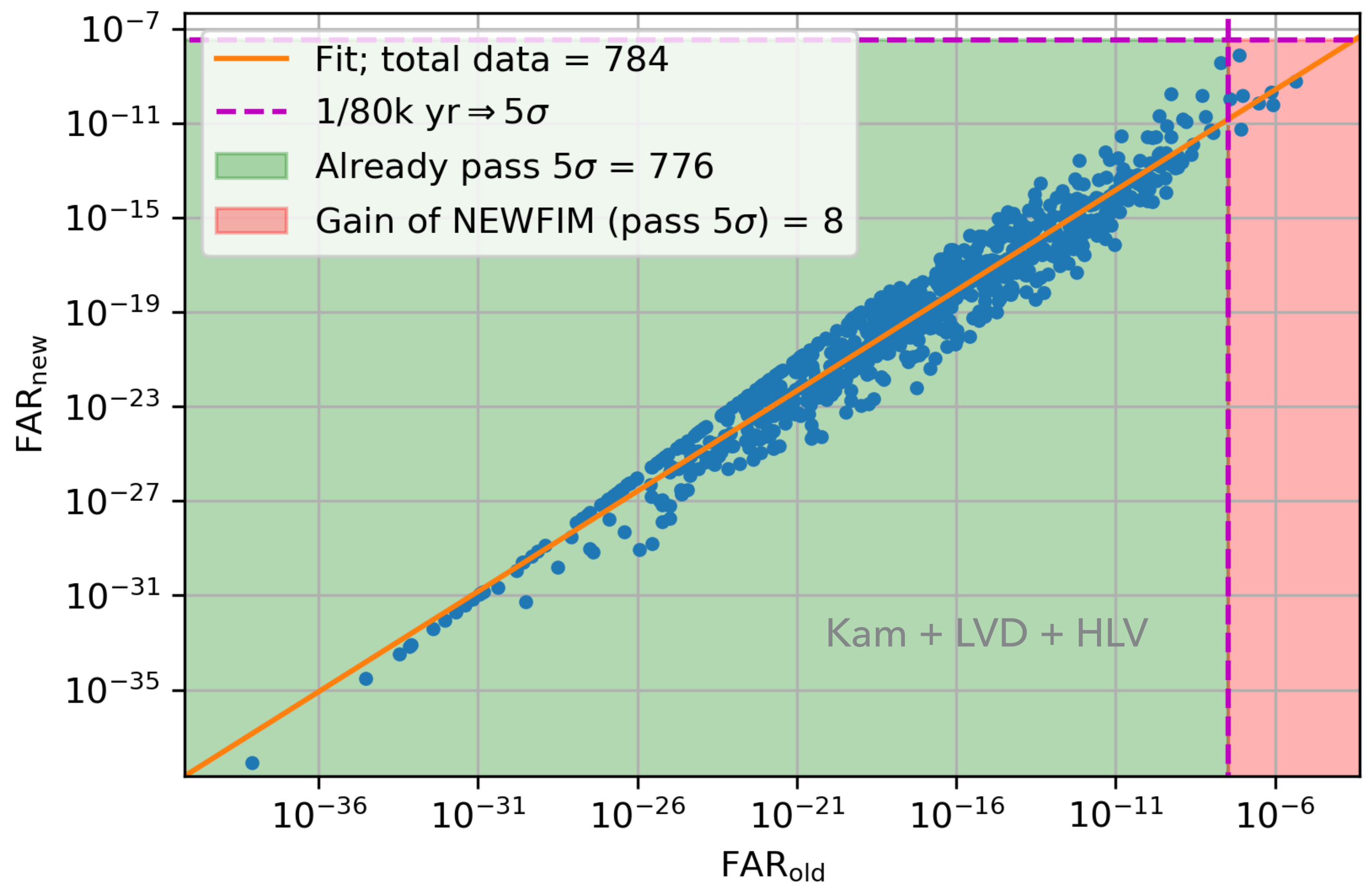

The recovered injections (784/2346) from cWB have FAR too low to be considered even as sub-thresholds

TABLE V: Efficiency (η) comparison of 1-parameter and our 2-parameter method for Figure 7 and 8. The first column points the specific network of detectors considered and the adopted emission models. The second column is after we impose the threshold on FAR of GW data (< 864/day). The third and last columns report the fraction of signals with a significance greater than 5σ (efficiency) with 1-parameter and 2-parameter methods.

Network & Type of Injections	Recovered $FAR_{GW} < 864/d$	η_{1param} $[> 5\sigma]$	η_{2param} $[> 5\sigma]$
HLV-KAM (Dim2-SN1987A)	784/2346= 33.4%	554/784= **70.7%**	650/784= **82.9%**
HLV-KAM-LVD (Dim2-SN1987A)	784/2346= 33.4%	776/784= **99.0%**	784/784= **100%**

GLOBAL EFFICIENCY OF 1-PARAM METHOD:
$33.4\% \times 99.0\,\% = 33.1\,\%$

GLOBAL EFFICIENCY OF 2-PARAM METHOD:
$33.4\% \times 100.0\,\% = 33.4\,\%$

OH, et.al. 2021 *in preparation*

CONCLUSIONS

- Multimessenger analysis strategy has been done by combining gravitational wave and low-energy neutrino data
- Gravitational wave analysis uses cWB pipeline in order to produce low-significant triggers
- The 2-parameter refined analysis on low-energy neutrino data has been introduced and it has been proven to increase neutrino candidates' significance
- Multimessenger analysis will increase sub-threshold GW triggers' significance

Virtual Meeting
PRIN NAT-NET
6 July 2021

ENHANCED SN AXION EMISSIVITY BY PIONIC PROCESSES

Alessandro MIRIZZI
(Bari Univ. & INFN Bari)

Based on a work in collaboration with Carenza, Fore, Giannotti and Reddy, PRL 126 (2021)7, 071102, arXiv:2010.02943

AXION EMISSION FROM A SN

[Burrows et al., PRD 39, 4 (1989), Brinkmann and Turner, PRD 34, 8 (1988), Keil, Janka et al, PRD 56, 4 (1997)...]

$$NN \to NNa$$

nucleon-nucleon bremsstrahlung

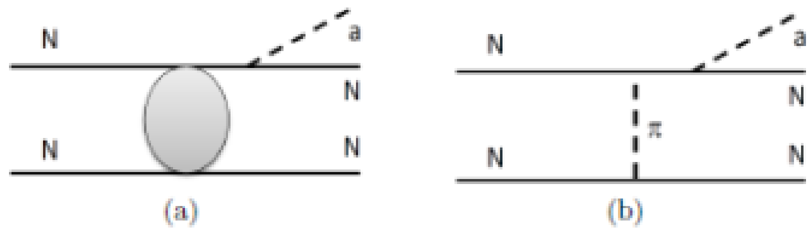

Bulk nuclear interaction   One pion exchange

$$\boxed{L_{aN} = \frac{g_{aN}}{2m_N}\overline{N}\gamma_\mu\gamma_5 N\partial^\mu a}$$

$$g_{aN} = C_N \frac{m}{f_a}$$

Non-degenerate energy-loss rate $\varepsilon_a = g_{aN}^2\, 2\times10^{39}\,\mathrm{erg\,g^{-1}\,s^{-1}}\rho_{15}T_{30}^{3.5}$

$$\begin{pmatrix} T_{30} = T/30\,\mathrm{MeV} \\ \rho_{15} = \rho/10^{15}\,\mathrm{g\,cm^{-3}} \end{pmatrix} \qquad \langle\rho_{15}\rangle \approx 0.4 \qquad \langle T_{30}^{3.5}\rangle \approx 1.4 \quad\Longrightarrow\quad g_{aN} < 9\times10^{-10}$$

SN 1987A AXION LIMITS FROM NU BURST DURATION

- Raffelt, Lect. Notes Phys. 741 (2008) 51 [hep-ph/0611350]
  Burst duration calibrated by early numerical studies
  "Generic" emission rates inspired by OPE rates
  $f_a > 4 \times 10^8$ GeV and $m_a < 16$ meV

- Chang, Essig & McDermott, JHEP 1809 (2018) 051 [1803.00993]
  Various correction factors to the emission rate, specific SN core models
  $f_a > 1 \times 10^8$ GeV and $m_a < 60$ meV [KSVZ, based on proton coupling]

- Bar, Blum & D'Amico, Is there a SN bound on axions?
  PRD 101 (2020) 12 [1907.05020]
  Alternative picture of SN explosion (thermonuclear event)
  Observed signal not PNS cooling.
  However the possible detection of NS 1987A in SN 1987A would disfavor alternative mechanisms [see Page et al., 2004.06078]

- Carenza, Giannotti, Gang, Fischer, Martinez-Pinedo & A.M. JCAP 10 (2019) 016 [1906.11855]
  Beyond OPE, specific SN core models
  $f_a > 4 \times 10^8$ GeV and $m_a < 15$ meV [KSVZ, based on proton coupling]

PION DENSITY IN SN CORE

[Fore and Reddy, PRC 101 (2020) 035809, 1911.02632 [astro-ph.HE]]

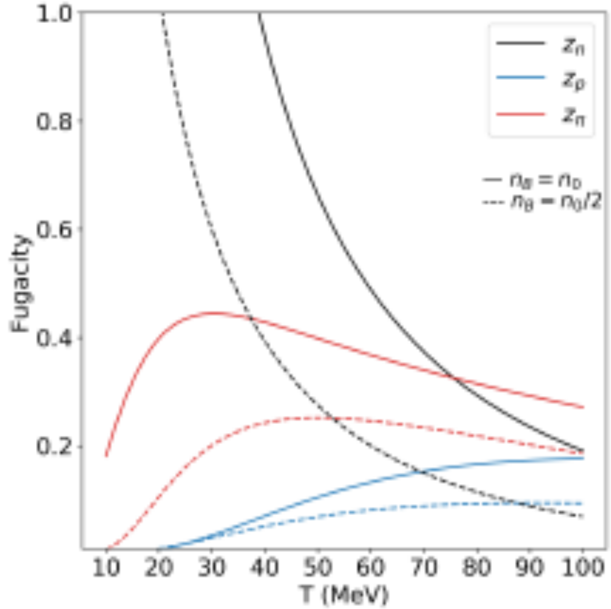

FIG. 3. Pion and nucleon fugacities in charge-neutral dense matter in β-equilibrium at $n_B = n_0$ (solid-curves) and $n_B = n_0/2$ (dashed-curves) are shown as function of temperature.

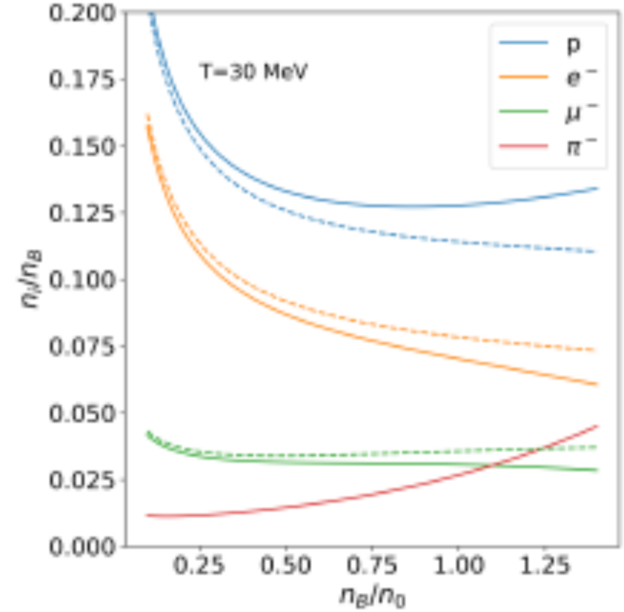

FIG. 2. Number fraction of charged particles at $T = 30$ MeV in β-equilibrium. Solid curves include pions and dashed curves only contain nucleons and leptons.

Around the saturation density $n_0 = 1.6 \times 10^{38} cm^{-3}$ the pion abundance can reach few % of the baryon one

AXION EMISSIVITY VIA PIONIC PROCESS

A population of π^- would lead to an additional channel of axions via Compton pionic process $\pi^- p \to n\, a$

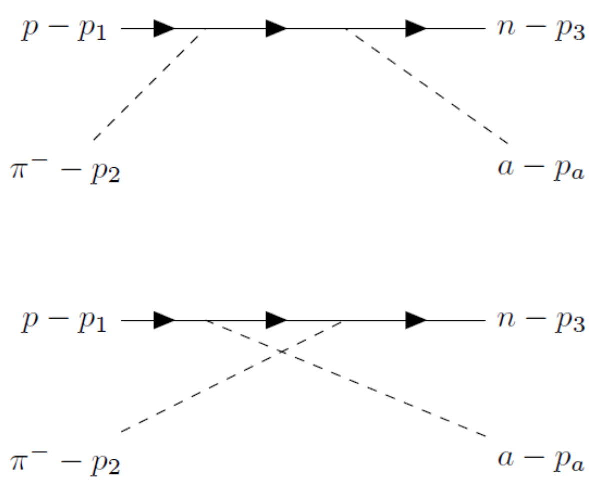

Initial investigations suggested that that the thermal pion population was too small for the pionic reactions to be competitive wrt to the NN process.

- Turner, Phys. Rev. D 45, 1066 (1992)
- Raffelt and Seckel, Phys. Rev. D 52, 1780 (1995) [astro-ph/9312019]
- Keil, Janka, Schramm, Sigl, Turner and Ellis, Phys. Rev. D 56, 2419 (1997) [astro-ph/9612222]

IMPACT ON AXION LUMINOSITY AND MASS BOUND

[Carenza, Fore, Giannotti, A.M., Reddy, 2010.02943]

- Axion emissivity

TABLE I: Axion emissivities Q_a in units of $10^{32}\,\mathrm{erg\,cm^{-3}\,s^{-1}}$ and luminosities L_a in units $10^{51}\,\mathrm{erg\,s^{-1}}$ for KVSZ model ($C_{ap} = -0.47\,; C_{an} = 0$) and $g_a = m_N/f_a = 10^{-9}$, for different post-bounce times.

t_{pb} (s)	ρ $(10^{14}\mathrm{g/cm^{-3}})$	T (MeV)	Y_π	Q_a^{NN} $(10^{32}\,\mathrm{erg\,cm^{-3}\,s^{-1}})$	Q_a^{π} $(10^{32}\,\mathrm{erg\,cm^{-3}\,s^{-1}})$	Q_a^{tot}/Q_a^{NN}	L_a $(10^{51}\,\mathrm{erg\,s^{-1}})$
1	1.45	37.07	0.011	1.37	4.63	4.38	4.0
2	2.08	38.93	0.016	3.28	8.87	3.70	8.10
4	3.10	40.56	0.027	9.08	15.87	2.75	16.63
6	3.65	39.91	0.034	12.92	14.99	2.16	18.61

Axion emissivity increased by a factor 4 due to pionic processes at t_{pb}= 1 s

- Axion Mass bound

Schematic SN model. T= 30 MeV, Y_p=0.3, ρ_{sat}= 2.6 x 10^{14} g/cm^3

TABLE II: Bound on the effective axion-nucleon coupling $\bar{g}_{aN}$ obtained using Eq. (13). The corresponding bound on m_a and f_a for KVSZ model with $C_{ap} = -0.47\,, C_{an} = 0$ are also shown.

ρ		$\bar{g}_{aN}$ $(\times 10^{-9})$	m_a (meV)	f_a $(\times 10^8$ GeV)
ρ_0	only NN	0.81	21.02	2.71
	$\pi N + NN$	0.46	11.99	4.75
$\rho_0/2$	only NN	0.93	24.11	2.36
	$\pi N + NN$	0.42	10.96	5.20

Axion mass bound strengthened by a factor 2 when πN processes are included

DETECTION PERSPECTIVES FOR SN AXION BURST

[Carenza, Fore, Giannotti, A.M., Reddy, 2010.02943]

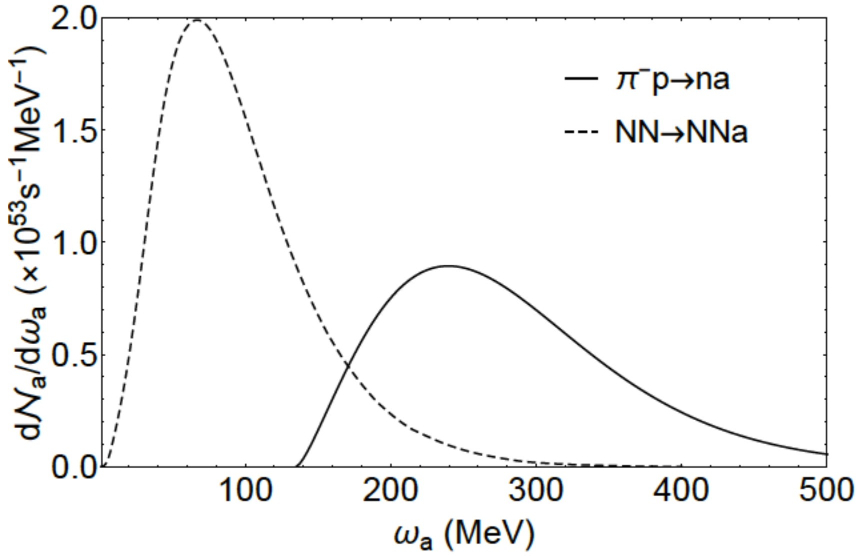

- πN process produces a harder axion spectrum (E ~ 200 MeV) with respect to the NN process
- High-energy axions would produce neutral and charged π in a water Cherenkov detector, due to processes a+ p → N + π
- For E ~ 200-300 MeV resonant enhancement of the a-N cross section due to Δ intermediate state

Simple estimation of the axion events

$$\sigma_{aN} = (F_\pi \,/ f_a\,)^2\, \sigma_{\pi N}$$

$$\sigma_{\pi N} \approx 100\, mbarn$$

→ 1000 pions !

@ $f_a = 10^9\, GeV$
(m_a=5.7 meV)
d_{SN}= 1 kpc
1 Mton detector

Intriguing possibility to be investigated

SN SIMULATIONS WITH PIONS

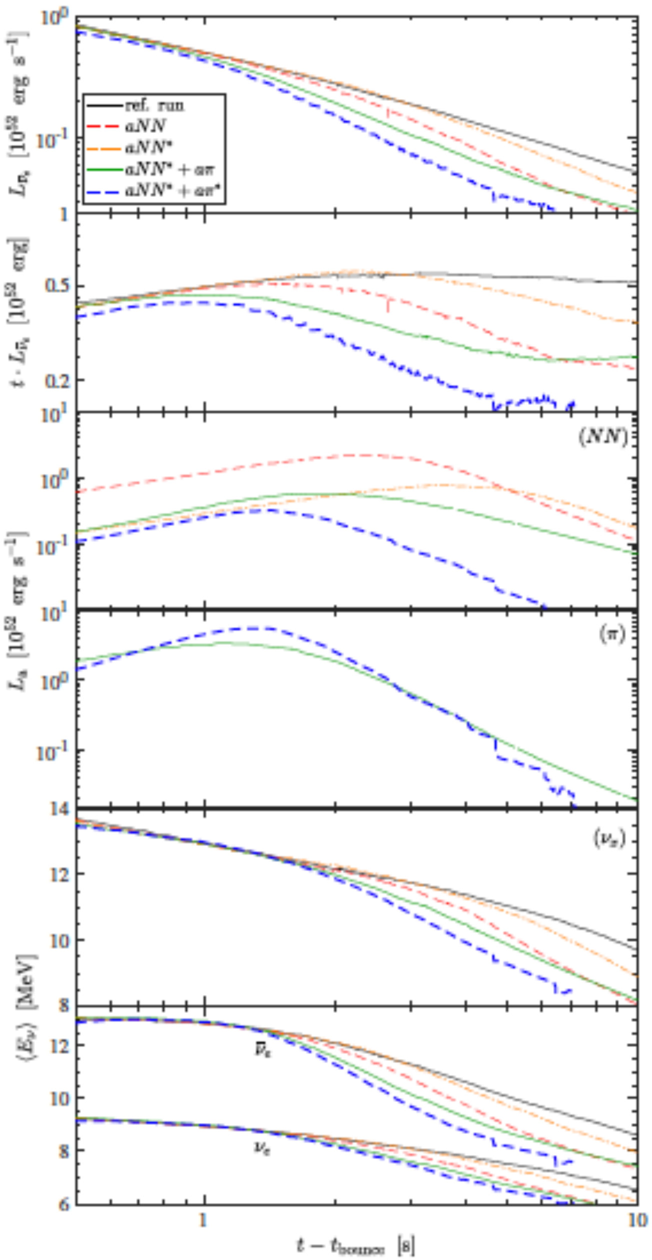

[Fischer, Fore, Reddy, Carenza, Giannotti, A.M. , work in progress]

g_{ap}=1.2 $\times 10^{-9}$ corresponding to bound from aNN*

- Remarkable differences wrt to reference case already at t_{pb}= 2 s
- Speed-up in SN neutrino cooling
- Pionic processes are the dominant channel of axion energy loss in SN

CONCLUSIONS

Core-collapse SNe represent powerful laboratories to constrain axions

- We perfomed a reliable calculation of the NN axion emissivity including relevant corrections beyond OPE
- We pointed out that pionic processes might strongly enhance axion emissivity
- We included self-consistently these processes in a SN simulation to determine the feed-back on the neutrino signal
- It is mandatory to investigate impact of axion energy-loss on the observable SN neutrino signal.

A Galactic SN is a lifetime opportunity for axions !

II PRIN NAT-NET MEETING
6 July 2021

Axion-like particles from Hypernovae

Giuseppe LUCENTE
Bari University "Aldo Moro"
INFN, Bari

Based on
A. Caputo, P. Carenza, G. L., E. Vitagliano, M. Giannotti, K. Kotake, T. Kuroda, A. Mirizzi
ArXiv 2104.05727 [hep-ph]

AXION-LIKE PARTICLES

ALPs interacting only with photons

$$\mathcal{L}_{a\gamma} = -\frac{1}{4} g_{a\gamma}\, a\, \tilde{F}^{\mu\nu} F_{\mu\nu} = g_{a\gamma}\, a\, \vec{E} \cdot \vec{B}$$

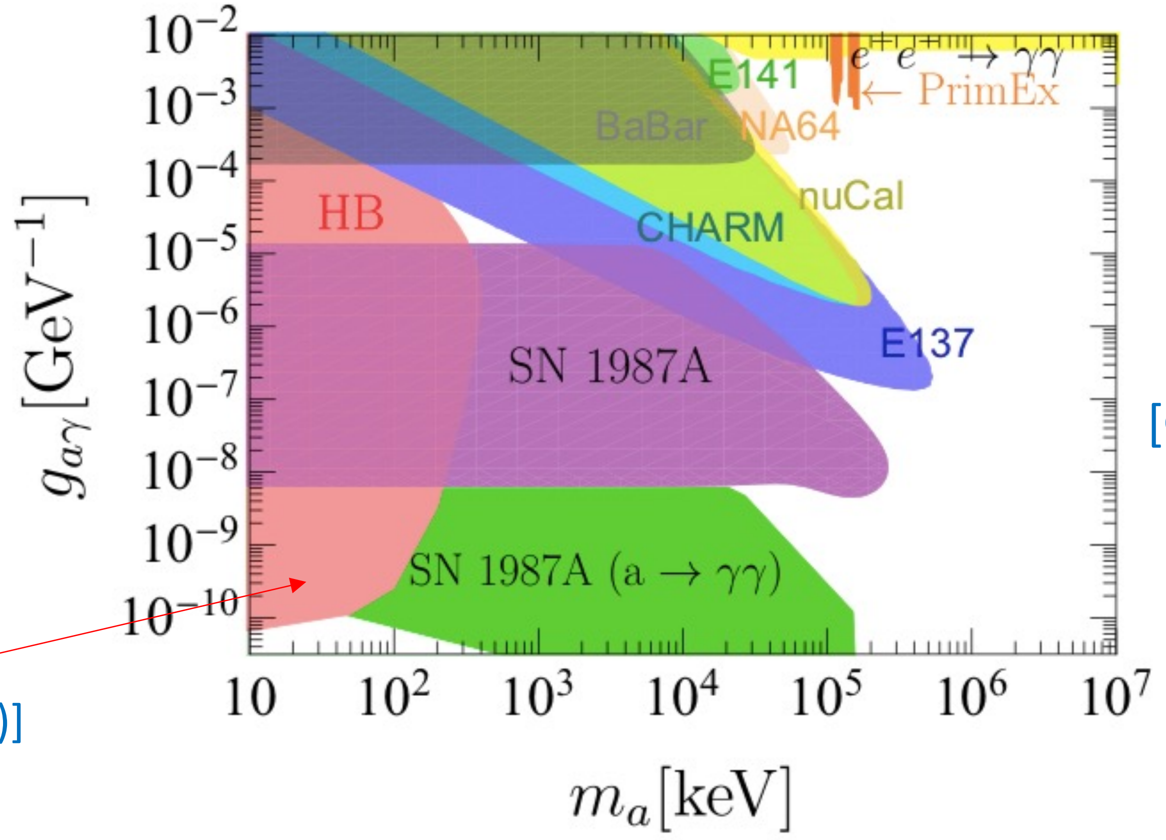

[G.L. et al., *JCAP* 12 (2020)]

[Carenza et al., PLB 809 (2020)]

MHD SUPERNOVAE

- Very energetic supernovae: magnetohydrodinamically-driven (MHD) explosion. [Burrows *et al.*, *ApJ* 664 (2007)]
- Recent development of MHD SN simulations in 2D [Matsumoto et al., MNRAS 499 (2020)] and 3D [Kuroda et al., APJ 896 (2020)]: ultra-strong magnetic fields $B \gtrsim 10^{15}$G in the SN core.
- Reference model: fully relativistic 3D magnetorotational core-collapse SN simulation of a 20 $M_{\odot}$ star [Kuroda, Astrophys.J. 906 (2021)]

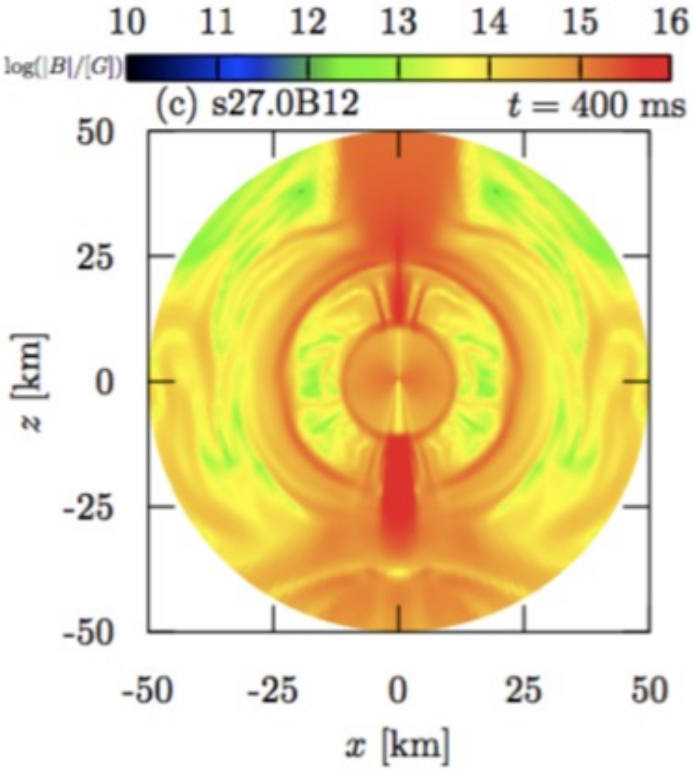

2D Model

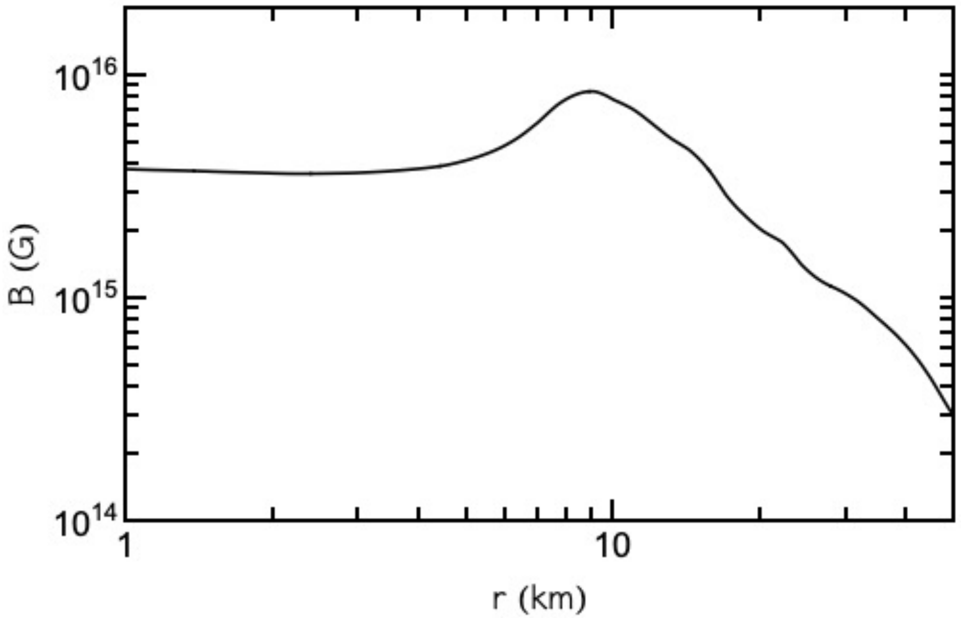

Angle averaged radial profile of B-field in our reference model at final time $t_{pb} = 370$ ms

PRIMAKOFF PROCESS

Photon-ALP conversion in the electric field of free protons in the SN core.

Production rate: [Di Lella, PRD 62 (2000); G.L. et al., *JCAP* 12 (2020)]

$$\Gamma_P = g_{a\gamma}^2 \frac{T\kappa_s^2}{32\pi} \frac{p}{\omega} F(p,k,\kappa_s)$$

$$F(p,k,\kappa_s) = \frac{[(k+p)^2+\kappa_s^2][(k-p)^2+\kappa_s^2]}{4kp\kappa_s^2} \ln\left[\frac{(k+p)^2+\kappa_s^2}{(k-p)^2+\kappa_s^2}\right] - \frac{(k^2-p^2)^2}{4kp\kappa_s^2} \ln\left[\frac{(k+p)^2}{(k-p)^2}\right] - 1$$

p and k ALP and photon momenta

Screening scale $\kappa_s^2 \approx \frac{4\,\pi\,\alpha\, n_p}{T}$ → Proton density

RESONANT PHOTON-ALP CONVERSIONS

Resonant ALP production in an external B field when the photon dispersion relation ω_0^T matches the ALP dispersion relation.

Production rate: [Caputo et al., *PRD* 101 (2020)]

$$\Gamma_B = \omega^2\, B_\perp^2\, g_{a\gamma}^2 \frac{\pi}{2\omega^2}\, \delta\left(\omega - \omega_0^T(k)\right)$$

- For ALPs $\omega = \sqrt{k^2 + m_a^2}$
- $\omega_0^T(k)$ depends on the plasma frequency ω_{pl}
- In a SN: $\omega_0^T \approx \sqrt{k^2 + \frac{3}{2}\omega_{pl}^2}$ when $k \gg \omega_{pl}$
- Resonance where $\omega_{pl}(r) \approx m_a$

Resonant region for $m_a = 5$ MeV

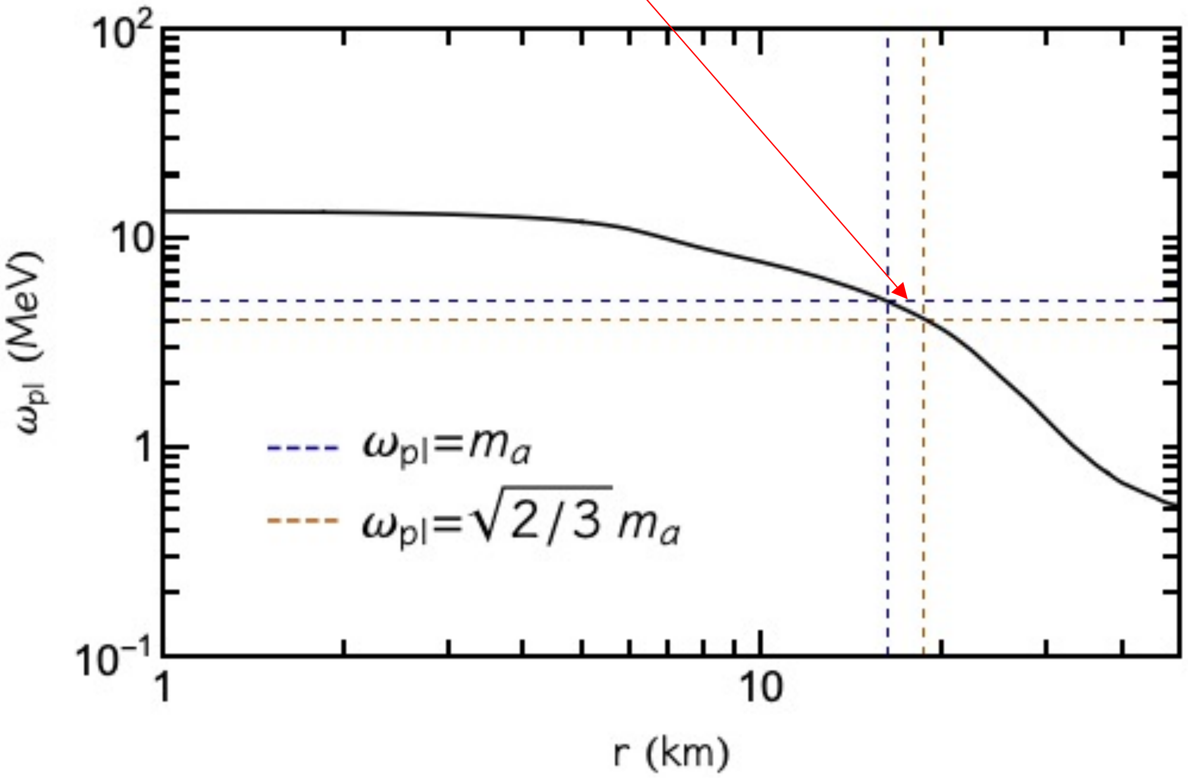

ALP LUMINOSITY

$$L_a = \int d^3\boldsymbol{r} \int \frac{d^3\boldsymbol{k}}{(2\pi)^3} \frac{2\,\Gamma\,\omega}{e^{\omega/T}-1} = \int d\omega\,\omega \frac{dN_a}{d\omega\,dt}$$

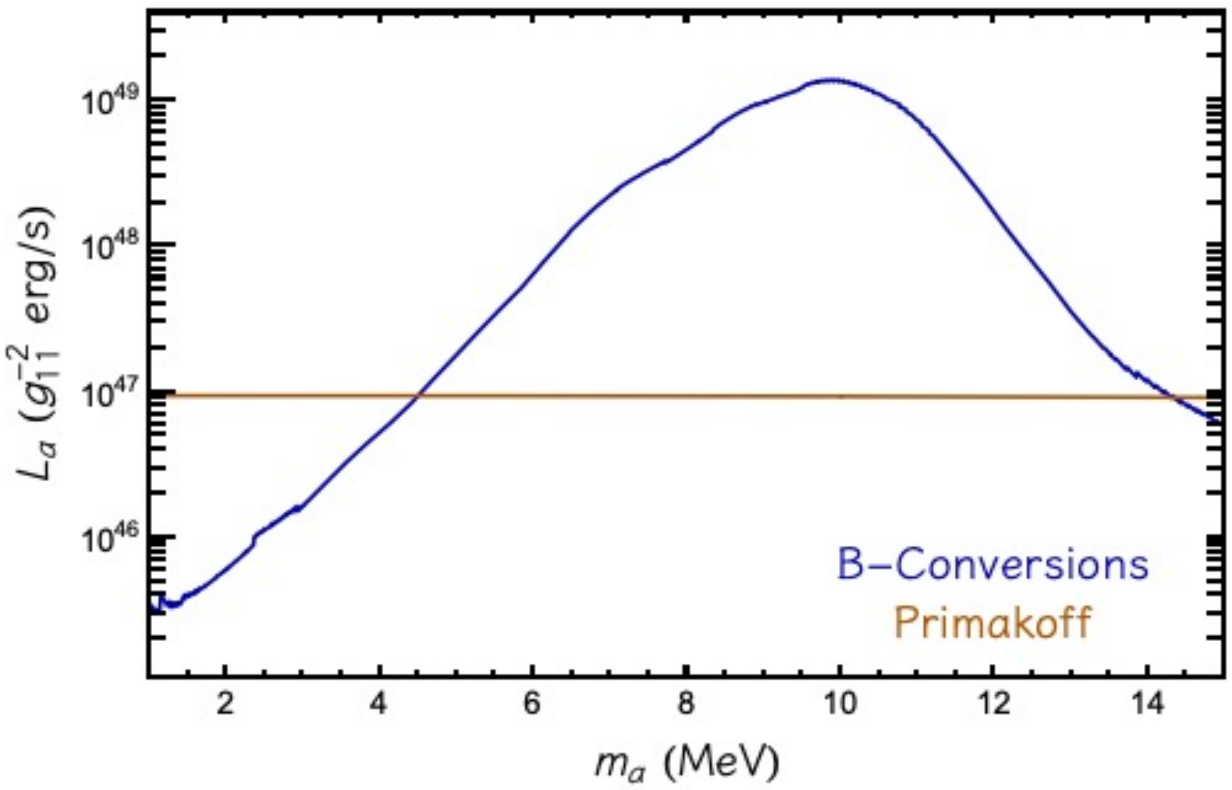

$$g_{11} = \frac{g_{a\gamma}}{10^{-11}\ \mathrm{GeV}^{-1}}$$

B-conversions dominant for $4 \lesssim m_a \lesssim 14$ MeV, $L_B \approx 100\ L_P$ at $m_a \approx 10$ MeV.

ALP FLUX

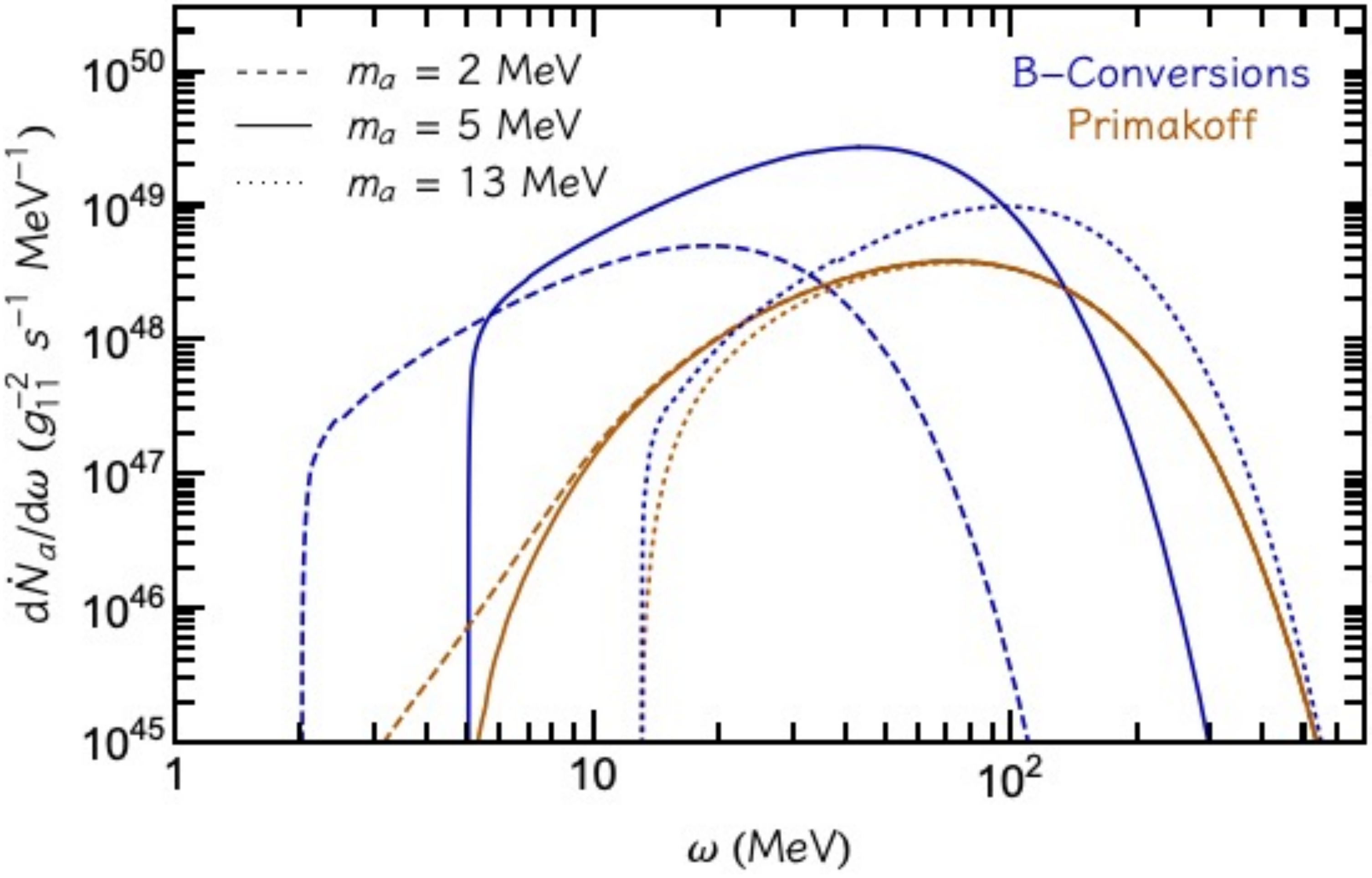

B-conversions dominate over Primakoff for $\omega \lesssim O\ (100)$ MeV.

DETECTION OF ALP-ORIGINATED PHOTONS

Gamma-ray flux from $a \to \gamma\gamma$: more energetic photons will arrive on Earth earlier.

$\tau_0 = 10^5$ s

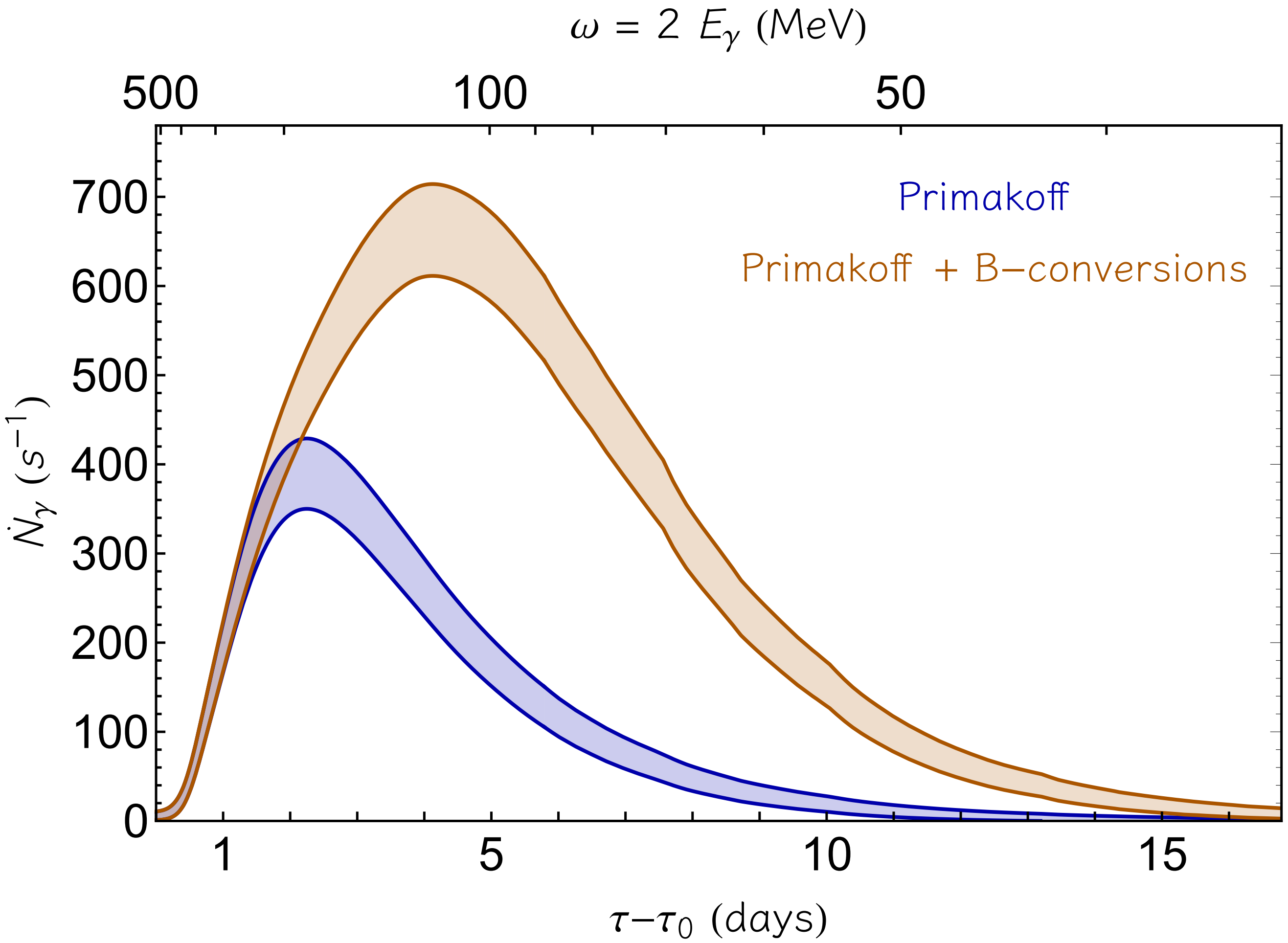

Evidence for:

1. Existence of ALPs
2. $m_a \approx 10$ MeV
3. B fields in SN core

Expected number of events per unit time detected by Fermi-LAT for $g_{a\gamma} = 10^{-11}$ GeV^{-1}, $m_a = 5$ MeV and $d_{SN} = 10$ kpc.

CONCLUSIONS

- Very energetic supernovae, such as hypernovae, may host intense magnetic fields in their core.
- These fields would trigger a resonant ALP production via photon conversion: dominant process for $m_a \sim O(10)$ MeV in SNe with $B \sim O(10^{15})$ G.
- Detection in Fermi-LAT of a photon flux originated by ALP decay: smoking gun for the existence of ALPs and the presence of ultra-strong magnetic fields in the SN core.

Thanks for your attention

PRIN MEETING

Could Starburst Galaxies Massively Produce High-Energy Neutrinos?

Starburst Galaxies Strike Back: a Multi-Messenger Analysis

ArXiv:2011.02483, AA, Marco Chianese, Damiano F.G. Fiorillo, Antonio Marinelli, Gennaro Miele, Ofelia Pisanti

Could nearby star-forming galaxies light up the point-like neutrino sky?

ArXiv: 2106.13248, AA, Marco Chianese, Damiano F.G. Fiorillo, Antonio Marinelli, Gennaro Miele

Antonio Ambrosone

University of Naples “Federico II”

Istituto Nazionale di Fisica Nucleare (INFN) sezione di Napoli

Why Starburst Galaxies?

https://hubblesite.org/image/3898/printshop

The Starburst Galaxy M82

Properties of SBGs

- High Star Formation Rate **(10-100 times higher than Milky Way)**
- They are abundant **(~10^4 — 10^5 Gpc^{-3})**
- Not very brilliant in gamma-rays **(only a few currently observed)**

Emission Properties of SBGs

dust, gas, ...

$$p + p \to \pi^+ \, \pi^- \, \pi^0 \ldots$$

p-p interaction is likely to occur when *density of gas higher than density of radiation* (for example in Starburst Galaxies)

- Generally, the SBGs are considered with the same properties of a ***prototype*** galaxy with "known" parameters (Peretti et al., **arXiv:1812.01996**, **arXiv:1911.06163**)

- In the calorimetric scenario, there are three main parameters:
  - Cut-off energy (p_{max})
  - Spectral index (α)
  - Rate of SuperNovae explosions

A new approach: Blending of Spectral Indexes

- We allow each starburst galaxy to have different a different spectral index

$$\left\langle \phi_{\nu,\gamma}(E|p^{\max},\alpha)\right\rangle_{\alpha} = \int \mathrm{d}\alpha\, \phi_{\nu,\gamma}(E|p^{\max},\alpha)\, p(\alpha)$$

$$p(\alpha) = \mathcal{N}(\alpha|4.2, 0.04)$$

- 12 SFGs and SBGs have been resolved in gamma-rays
  Ajello et al., ***arXiv:2003.05493***

Larger contribution around 100 TeV! Potentially, It could alleviate the Tension between neutrino and gamma-ray data when using a hadronic model to explain IceCube observations.

ArXiv:2011.02483

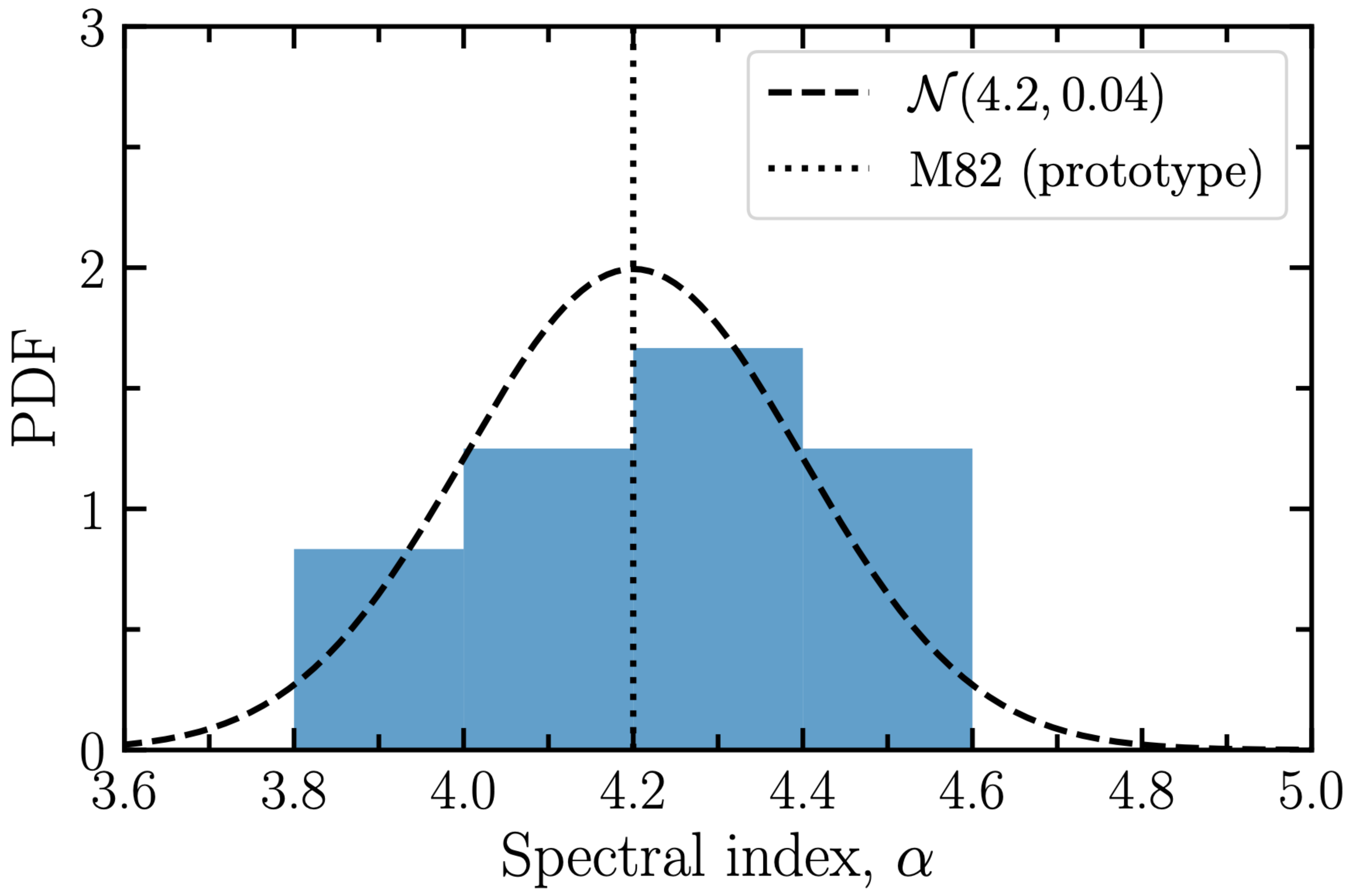

ArXiv:2011.02483

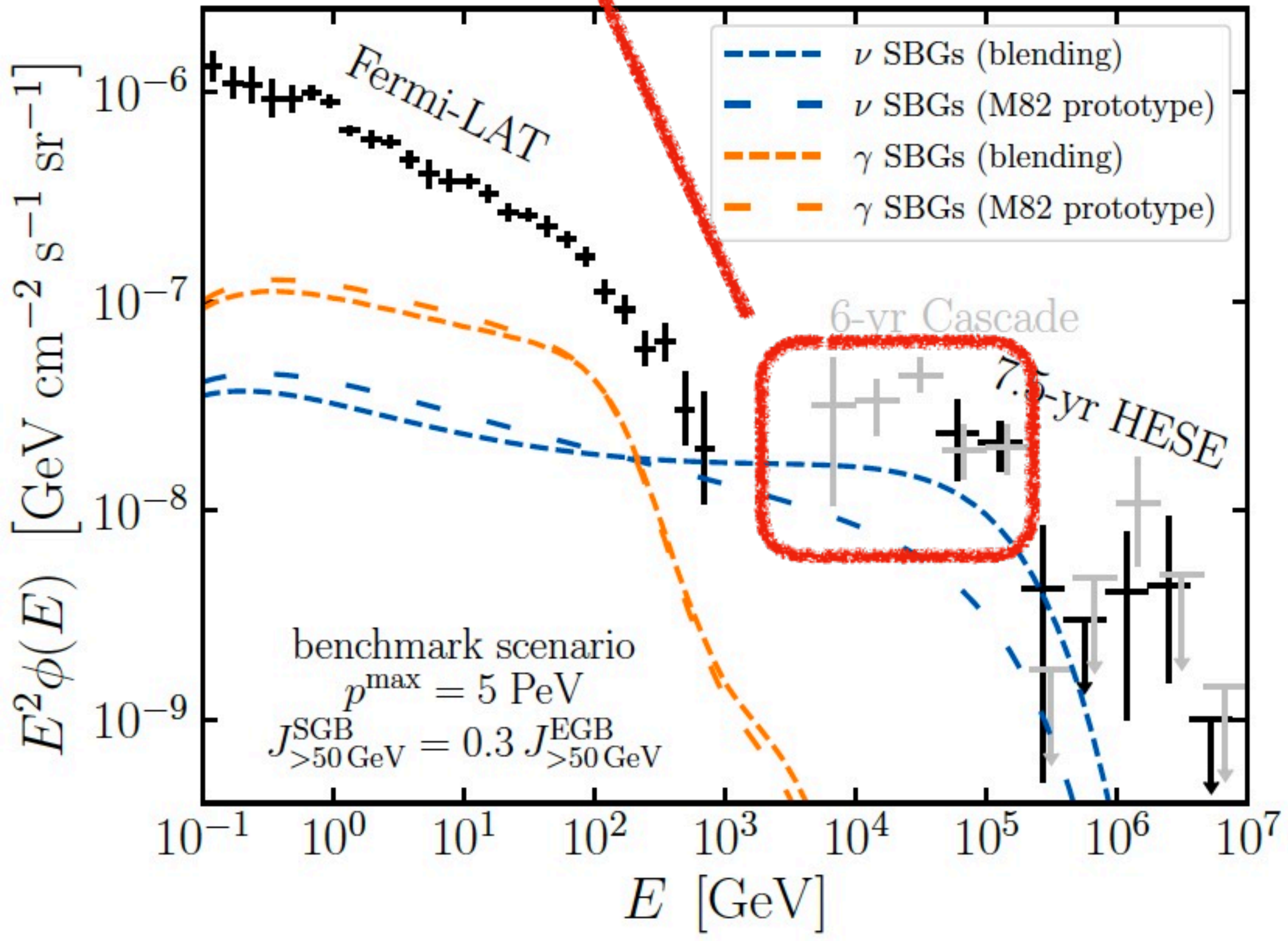

Results: Comparison between “Blending” and “Prototype”

- We performed a multi-component fit

The Gamma-Ray Contributions:
1. **SBGs**
2. **Blazar + Electromagnetic Cascades**
3. **Radio Galaxies**

For Blazars and Radio Galaxies, we used the estimations given by Ajello et al. 2015 **(ArXiv: 1501.05301)**

The Neutrino Contributions:
1. **SBGs**
2. **Blazars**

For Blazars, we used the estimations given by Palladino et. Al 2019 **(ArXiv:1806.04769)**

Main Result

ArXiv:2011.02483

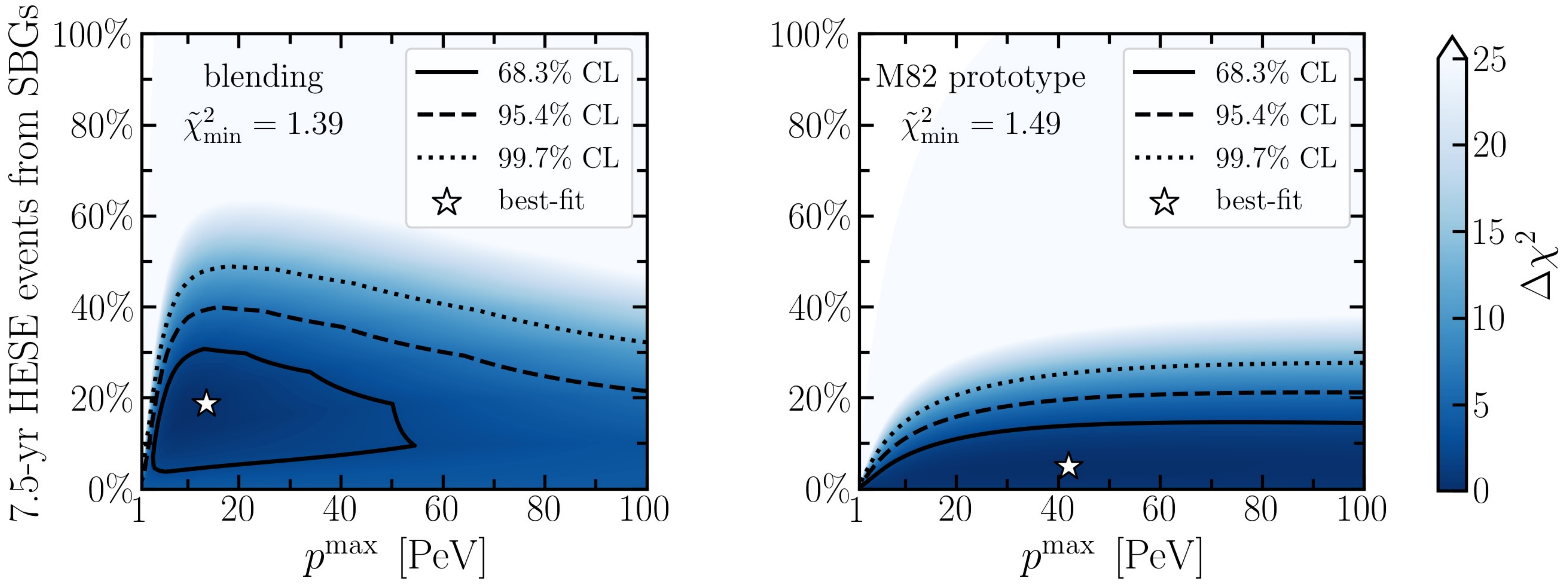

~ **Non-Zero SBG component at 68% Confidence Level**

~ **Preferred smaller values of the maximum energies for injected CRs:** $p^{max} < 50$ **PeV**

Could Neutrino Telescopes Observe SFGs and SBGs as point-like Sources?

We have to take into account the deep Universe $(z \sim 4-5)$ to explain a big part of IceCube's Measurements

What About Nearby Sources? Could they be Observed in the near future?

ArXiv: 2106.13248

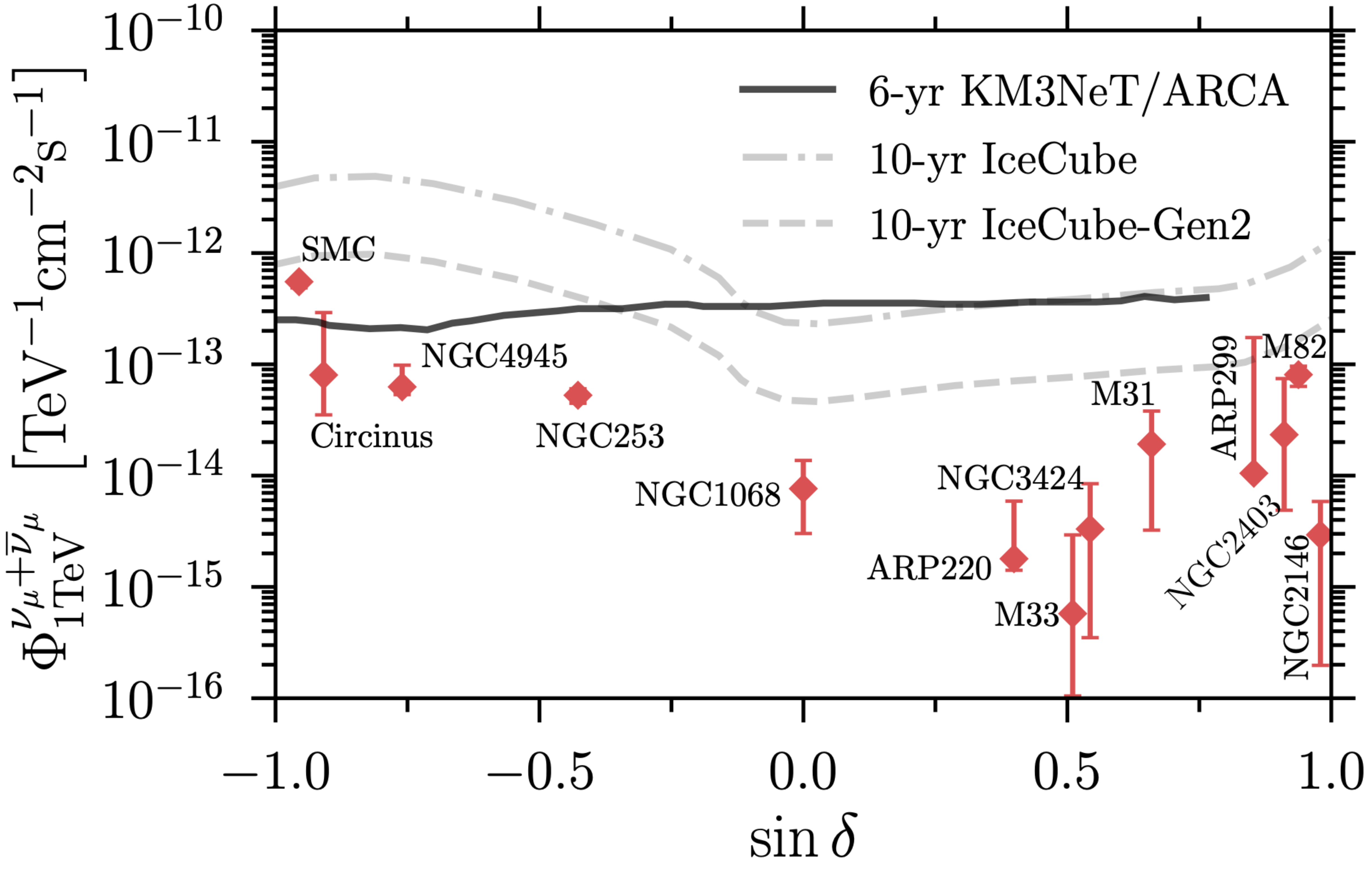

Conclusions

★ SBGs could play an important role for explaining the measured Astrophysical Neutrino Flux.

★We show how using the spectral behaviour of a new sample of Fermi-LAT SBGs increases the full-sky neutrino expectation at 100 TeV.

★ The reported multi-messenger study that considers gamma-ray EGB and neutrino HESE and cascades samples suggests a Pmax below tens of PeVs.

★In the Near future, some of the Known SFGs and SBGs could be observable with the upcoming neutrino telescopes

Unified thermal model for $p\gamma$ neutrino production in astrophysical sources

Damiano F. G. Fiorillo

Università degli studi di Napoli "Federico II"
INFN, Napoli

Based on
D. Fiorillo, A. Van Vliet, S. Morisi, W. Winter, arXiv:2103.16577 (accepted at JCAP)
D. Fiorillo, K. Satalecka, I. Taboada, C. F. Tung, arXiv:2105.14043 (accepted at ApJ)

Neutrinos as astrophysical messengers

Two production mechanisms for neutrinos

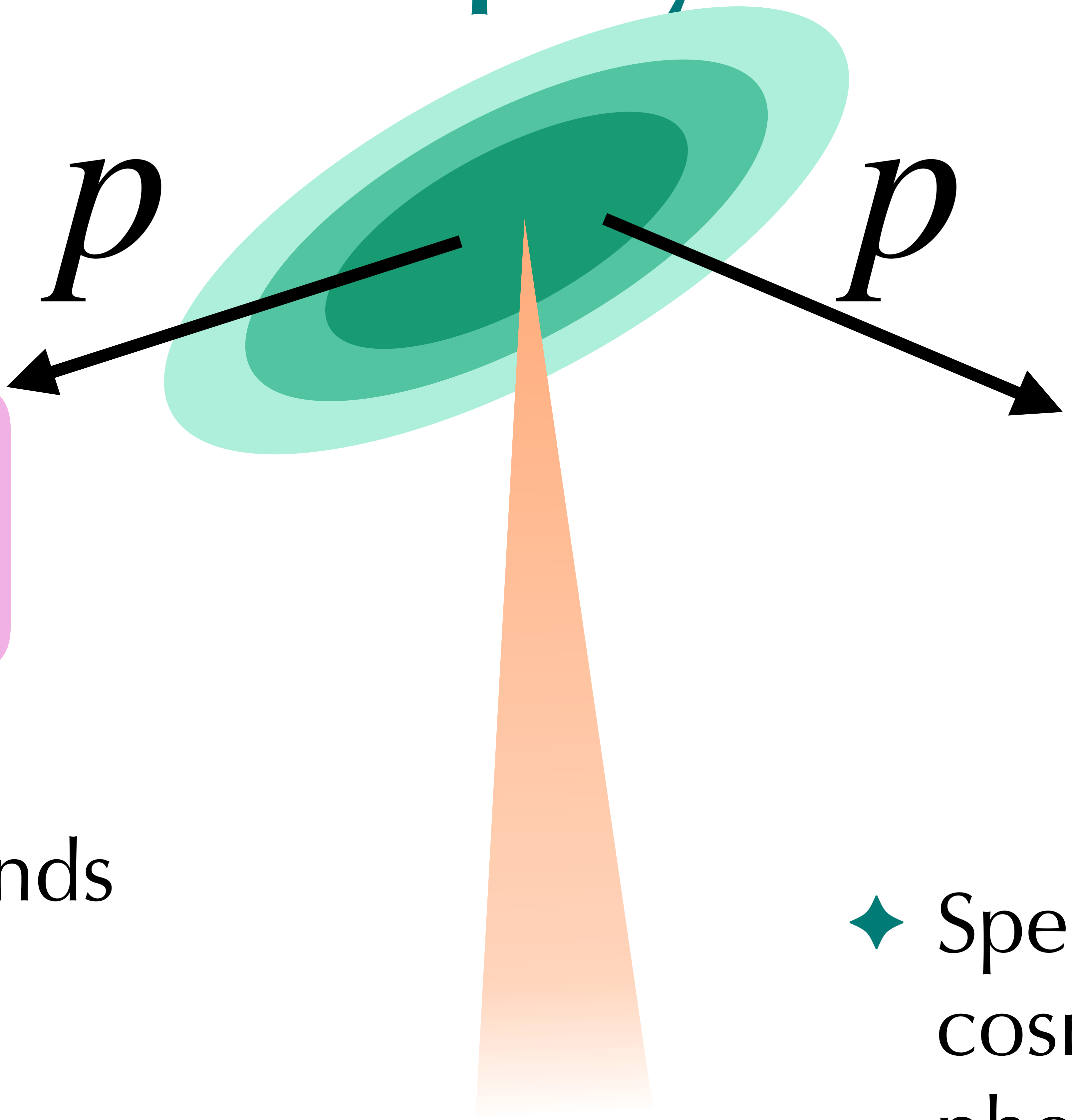

Proton target
(interstellar or intergalactic gas,…)

pp

- Spectral shape depends only on cosmic-ray spectrum
- Typically power law between 1 GeV and the maximum proton energy

Photon target
(synchrotron photons, infrared light, …)

$p\gamma$

- Spectral shape depends both on cosmic-ray spectrum and photon spectrum
- Typically broken power law, but hard to capture in general

Neutrinos as astrophysical messengers

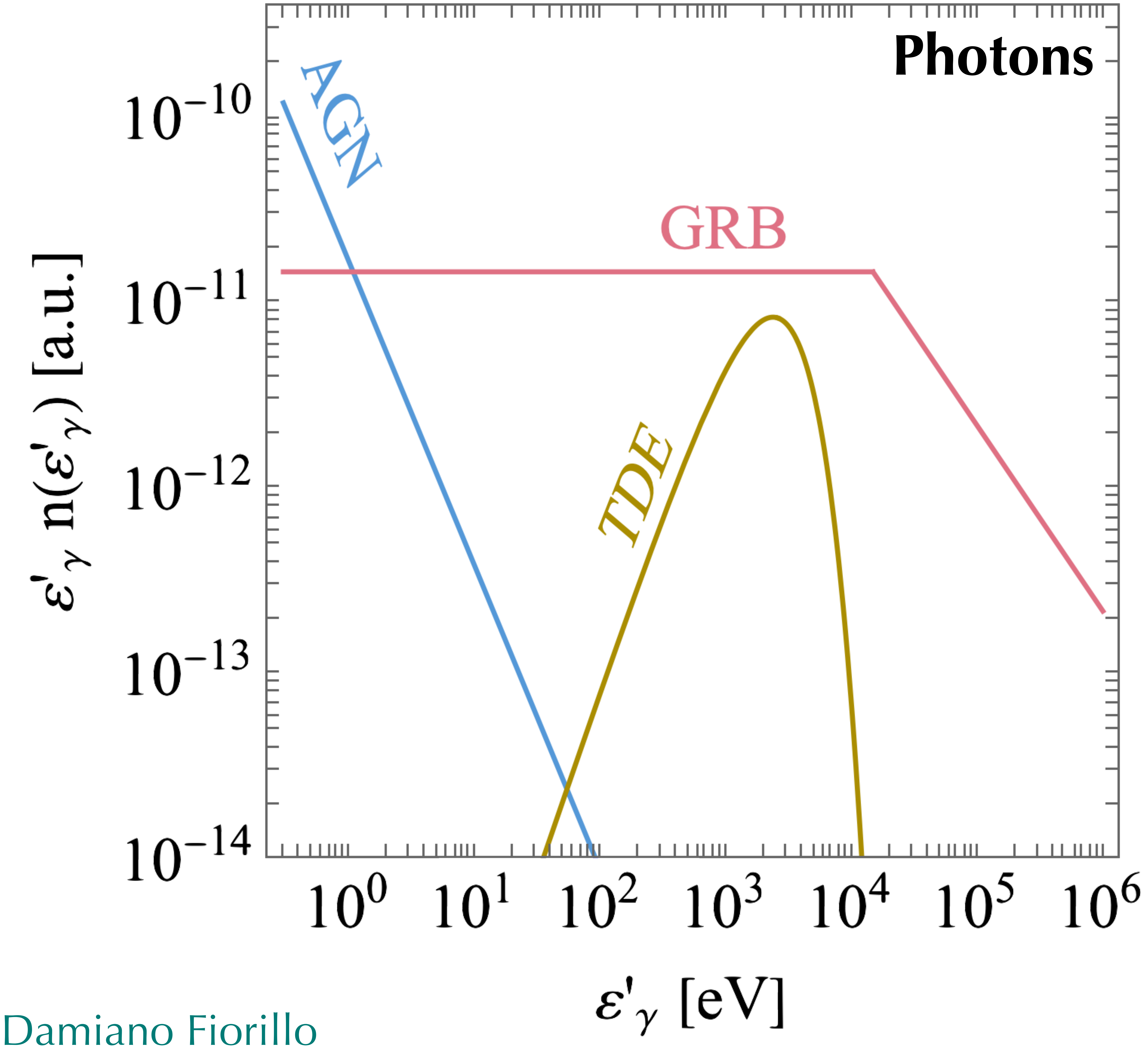

How do we capture the full variety in a unified way?

AGN: Gao et al., 2017 (Stecker et al., Atoyan et al., Alvarez-Muniz et al., Kimura et al., Rodrigues et al., Petropoulou et al., Murase et al., …)

GRB: Baerwald et al., 2012 (Waxman et al., Bottcher et al., Vietri et al., Guetta et al., Dermer et al., Meszaros et al., Murase et al., Hummer et al., Ando et al., …)

TDE: Winter et al., 2021 (Murase et al., Dai et al., Biehl et al., Zhang et al., …)

Typically broken power law, but hard to capture in general

Thermal model

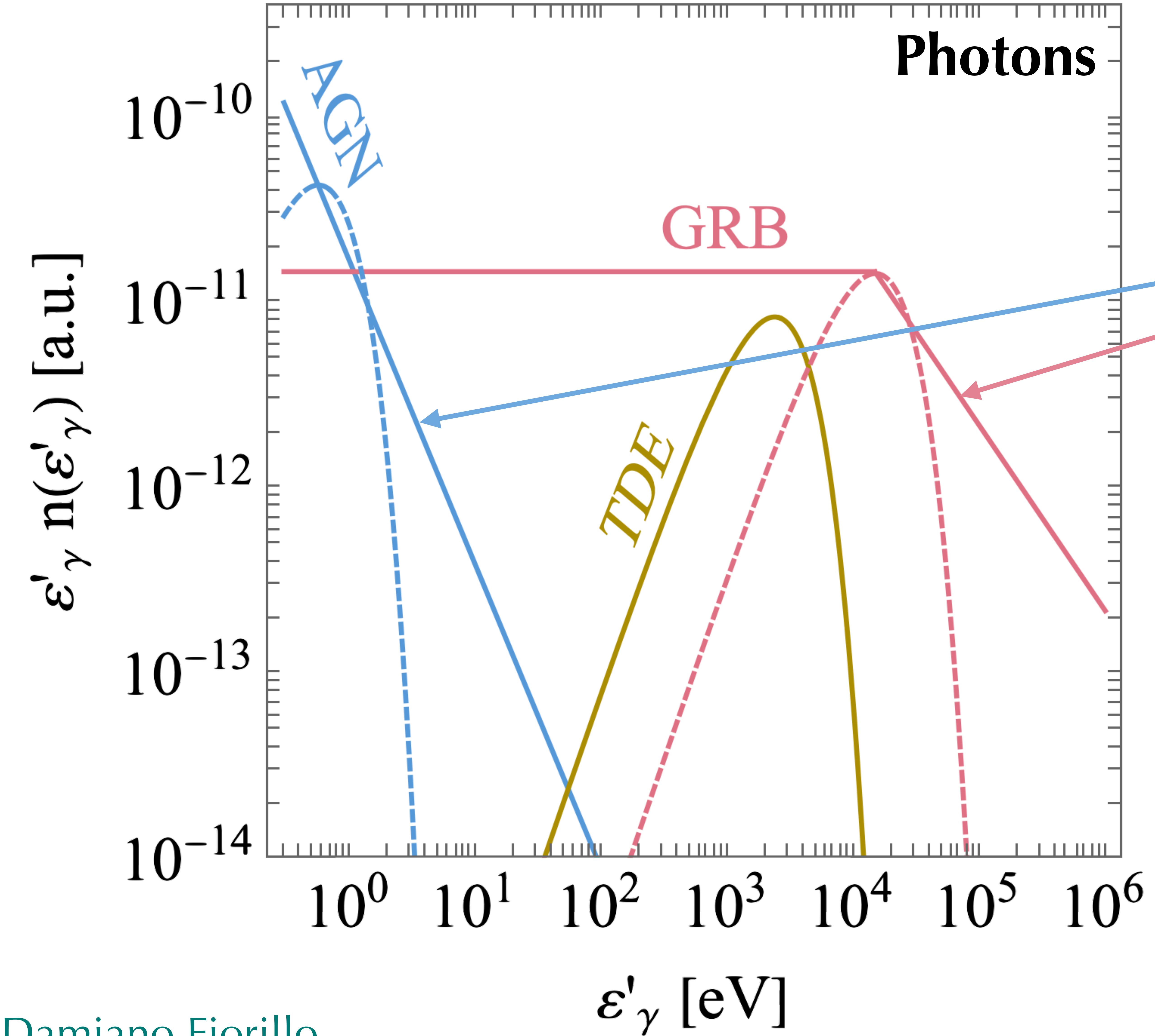

Idea: replace by thermal spectra peaked at the energy most contributing

Can capture neutrino spectral shape, of course not suitable for photon production!

Thermal model

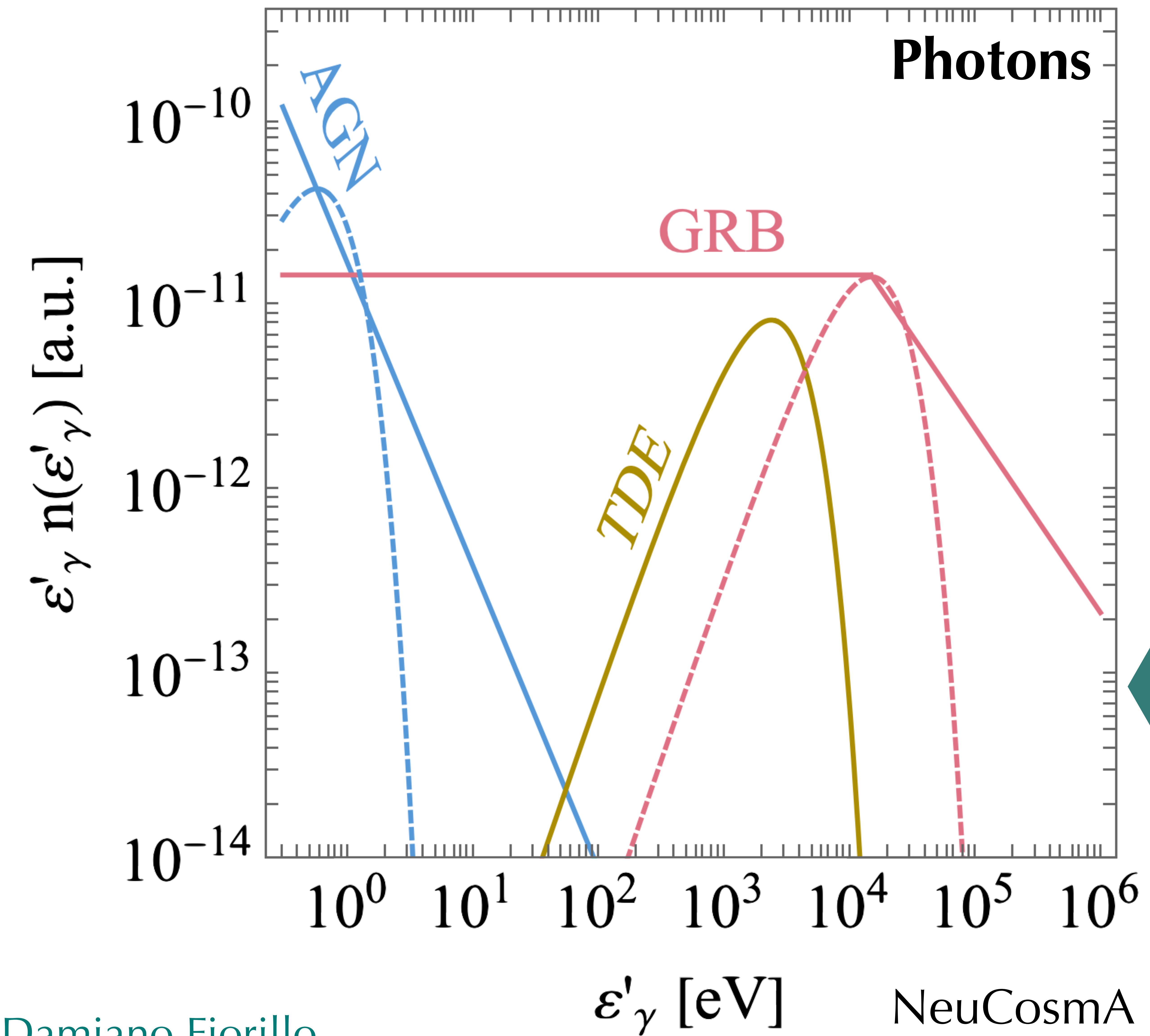

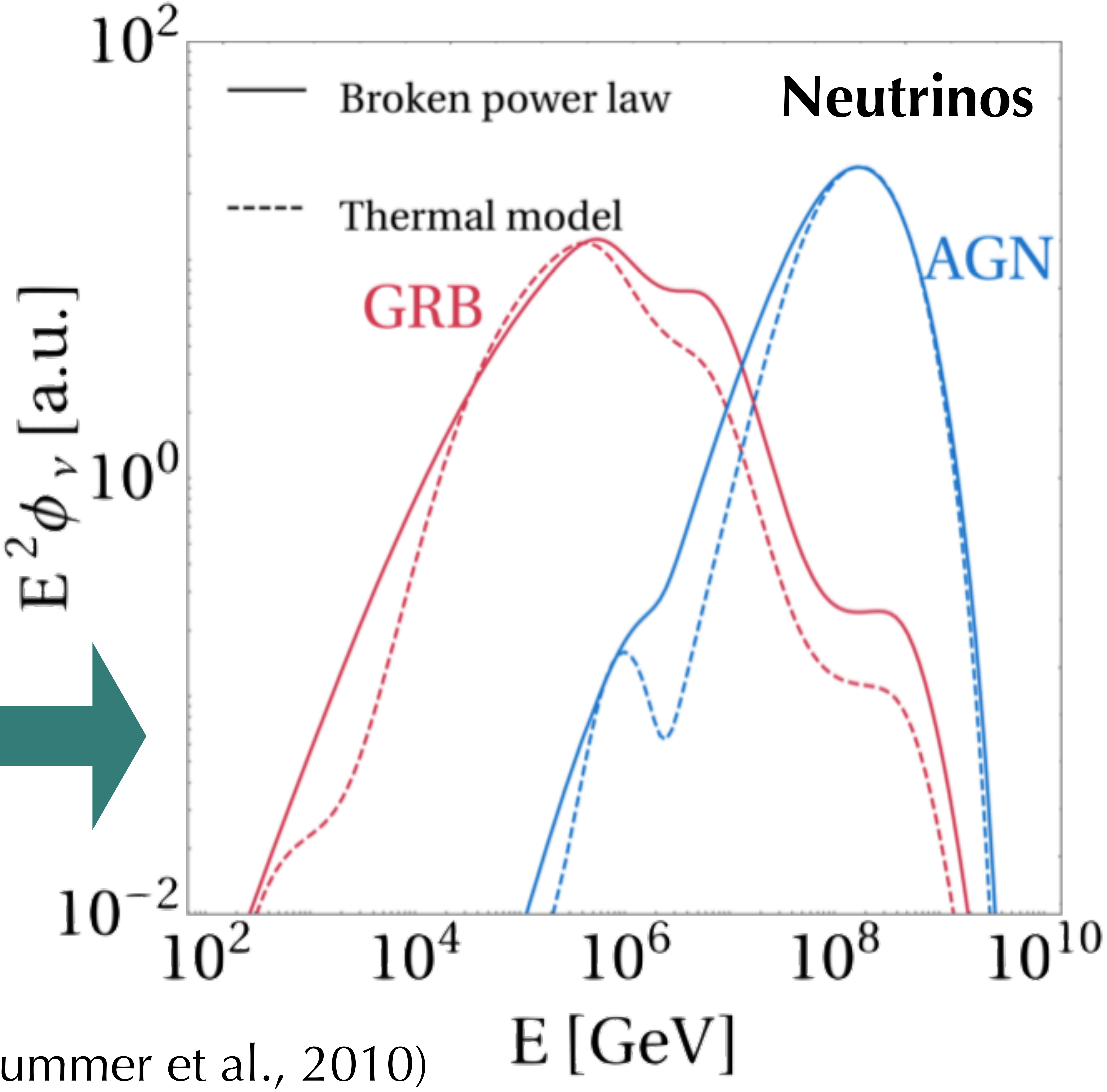

NeuCosmA (Hummer et al., 2010)

Thermal model

Cosmic-ray spectrum

Photon target

Max. p energy depends on:
R' source size
B' magnetic field
(assume maximal efficiency for acceleration)

Depends on:
T' photon temperature

Neutrino spectrum

Cooling of secondaries in magnetic field B'

Boost in the Earth frame with a Doppler factor Γ

Parameters: R', B', T', Γ

Follow-up program

- Imaging Air Cherenkov Telescopes (IACT) look in the direction of the neutrino
- Alert program led to the discovery of TXS0506+056
- For TXS the flare lasted hundreds of days

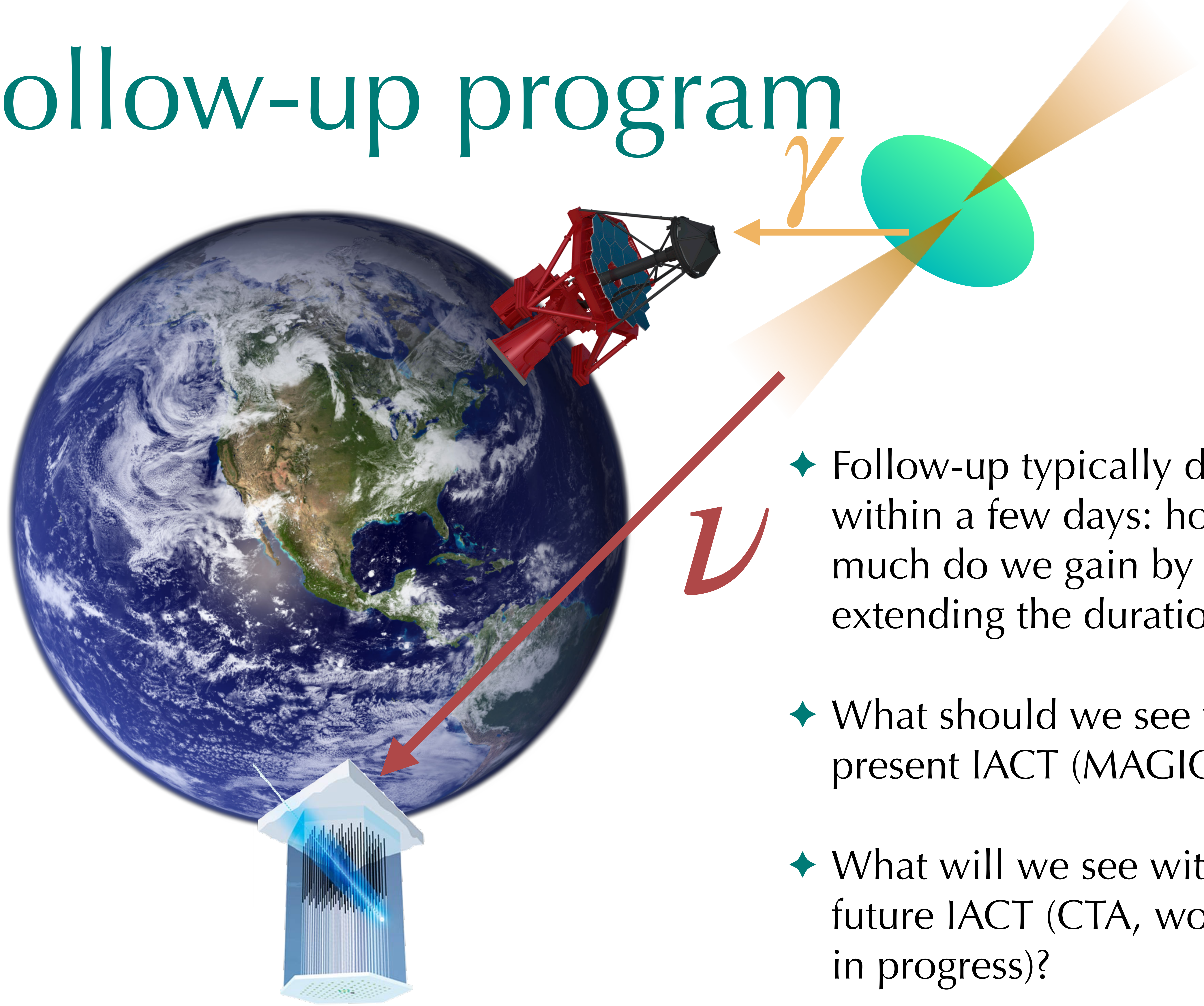

- Follow-up typically done within a few days: how much do we gain by extending the duration?
- What should we see with present IACT (MAGIC)?
- What will we see with future IACT (CTA, work in progress)?

Results

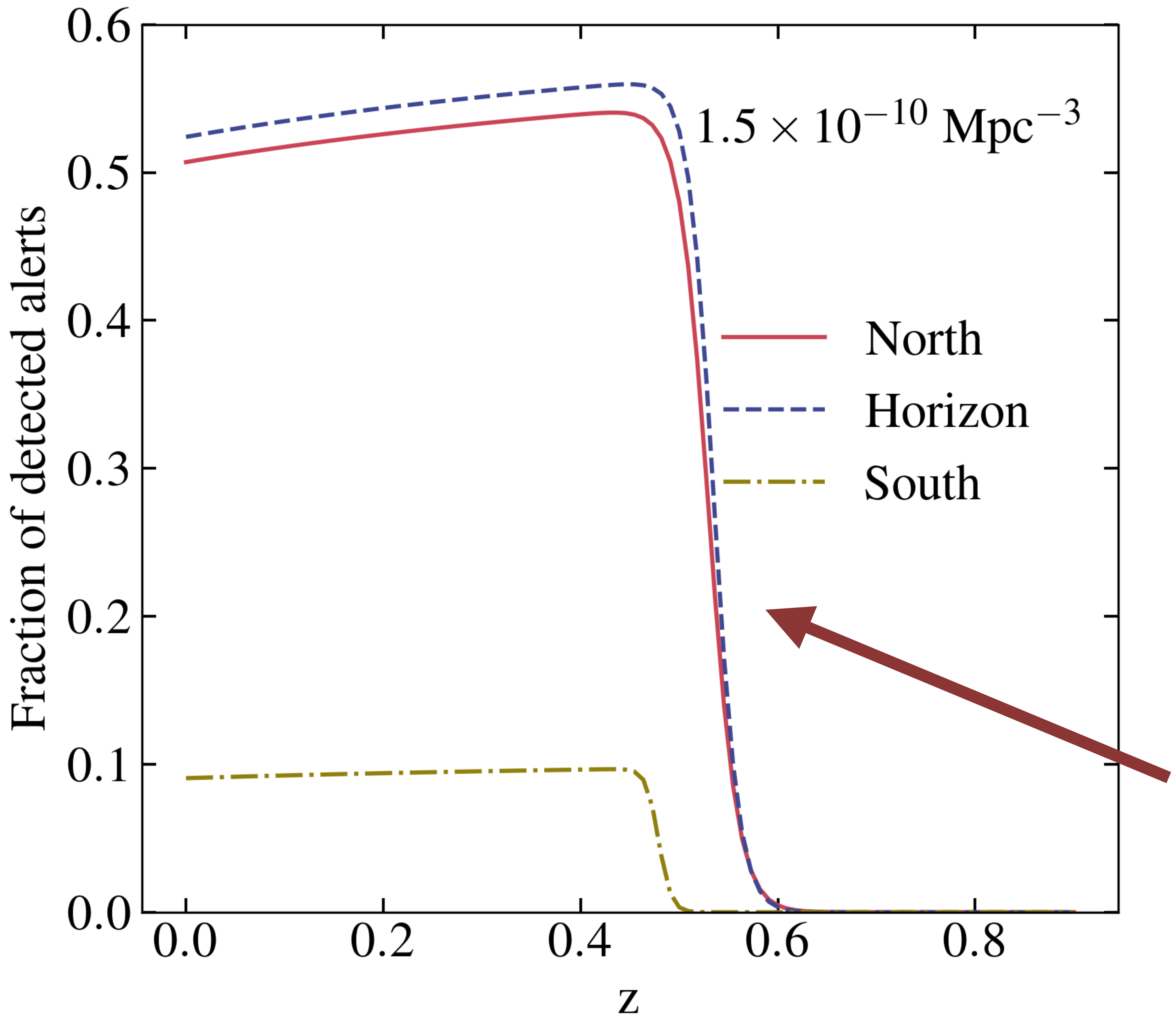

EBL-opaque!

How many IceCube alerts can MAGIC see?

Redshift is the critical factor

MAGIC should detect about 1.5 astrophysical alerts per year

Conclusions

- **Multimessenger emission** (γ, ν) can probe $p\gamma$ sources, but it requires flexible models
- **Thermal model** can describe $p\gamma$ production in a unified framework with four parameters: R', B', T', Γ
- **ν and γ emission** from TXS-like blazars can be tested by follow-up program in 30 days, possibly leading to 1.5 alerts per year